GEOPHYSICS, VOL. 82, NO. 4 (JULY-AUGUST 2017); P. WA67–WA81, 14 FIGS., 2 TABLES.
10.1190/GEO2016-0632.1

An acoustic eikonal equation for attenuating orthorhombic media

Qi Hao[1] and Tariq Alkhalifah[2]

ABSTRACT

Attenuating orthorhombic models are often used to describe the azimuthal variation of the seismic wave velocity and attenuation in finely layered hydrocarbon reservoirs with vertical fractures. In addition to the P-wave related medium parameters, S-wave parameters are also present in the complex eikonal equation needed to describe the P-wave complex-valued traveltime in an attenuating orthorhombic medium, which increases the complexity of using the P-wave traveltime to invert for the medium parameters in practice. We have used the acoustic assumption to derive an acoustic eikonal equation that approximately governs the complex-valued traveltime of P-waves in an attenuating orthorhombic medium. For a homogeneous attenuating orthorhombic media, we solve the eikonal equation using a combination of the perturbation method and Shanks transform. For a horizontal attenuating orthorhombic layer, the real and imaginary parts of the complex-valued reflection traveltime have nonhyperbolic behaviors in terms of the source-receiver offset. Similar to the roles of normal moveout (NMO) velocity and anellipticity, the attenuation NMO velocity and the attenuation anellipticity characterize the variation of the imaginary part of the complex-valued reflection traveltime around zero source-receiver offset.

INTRODUCTION

The attenuation of seismic wave propagation in reservoir rocks is closely linked to permeability, fluid content, and saturation (e.g., Winkler and Nur, 1982; Berryman, 1988; Batzle et al., 2006). The effective property of fluid-saturated reservoirs with aligned fractures exhibits velocity and attenuation anisotropy together, which may be described by a frequency-dependent attenuating anisotropic medium (e.g., Chapman, 2003, 2009; Jakobsen and Chapman, 2009). Laboratory and field observations have revealed that anisotropic attenuation is a common phenomenon for wave propagation in reservoir rocks (Tao and King, 1990; Carter and Kendall, 2006; Best et al., 2007; Clark et al., 2009; Behura et al., 2012; Shekar and Tsvankin, 2012; Zhubayev et al., 2016). The theory of wave propagation in attenuating media is systematically presented by Borcherdt (2009) and Carcione (2015, pp. 63–229).

Attenuating orthorhombic models may be used to describe the azimuthal variation of velocity and attenuation in finely layered hydrocarbon reservoirs with vertical fractures. Similar to an elastic orthorhombic medium, an attenuating orthorhombic medium includes three orthogonal symmetry planes. Besides, the symmetry of the imaginary part of the complex-valued stiffness matrix coincides with that of the real part of this matrix (Zhu and Tsvankin, 2007). In each of the symmetry planes, the homogeneous plane-wave propagation exhibits transverse isotropy in the aspects of phase velocity and attenuation coefficients, in which the term "homogeneous" means that the real and imaginary parts of a complex-valued wave vector are parallel to each other (e.g., Červený and Pšenčík, 2005a, 2005b, 2006; Zhu and Tsvankin, 2006, 2007). An attenuating orthorhombic media may be parameterized by a combination of Tsvankin's (1997) notation and Zhu and Tsvankin's (2007) notation (Appendix A), where Tsvankin's (1997) notation describes the velocities of the homogeneous plane waves in a nonattenuating background of an attenuating anisotropic medium, which corresponds to the real part of the stiffness coefficients; Zhu and Tsvankin's (2007) notation describes the attenuation coefficients of homogeneous plane waves in attenuating orthorhombic media. In addition to Zhu and Tsvankin's (2007) notation, Vavryčuk (2009) and Rasolofosaon (2010) propose two different weak anisotropy-attenuation notations to describe the attenuation of waves in generally attenuating anisotropic media.

The time-harmonic wave traveltime in attenuating media is generally complex valued. The complex-valued traveltime is governed

First presented at the 17th International Workshop on Seismic Anisotropy. Manuscript received by the Editor 30 November 2016; revised manuscript received 4 March 2017; published online 7 June 2017.
[1]Norwegian University of Science and Technology (NTNU), Department of Petroleum Engineering and Applied Geophysics, Trondheim, Norway. E-mail: xqi.hao@gmail.com; qi.hao@ntnu.no.
[2]King Abdullah University for Science and Technology (KAUST), Physical Science Division, Thuwal, Saudi Arabia. E-mail: tariq.alkhalifah@kaust.edu.sa.

by the complex eikonal equation, the form of which is similar to the real eikonal equation in nonattenuating media (Červený and Pšenčík, 2009). From the point of view of ray theory, the real and imaginary parts of the complex-valued traveltime of a time-harmonic ray control the phase and the attenuation due to energy absorption in an attenuating anisotropic medium (e.g., Gajewski and Pšenčík, 1992; Vavryčuk, 2007, 2010), respectively. The suggested approaches to invert for the quality factor, such as the spectral-ratio method (e.g., Dasgupta and Clark, 1998) and the frequency-shift method (e.g., Quan and Harris, 1997), naturally use the imaginary part of the complex-valued traveltime. Similar techniques have been applied to estimate the attenuation parameters of an attenuating anisotropic medium (Zhu et al., 2007; Behura and Tsvankin, 2009; Clark et al., 2009; Shekar and Tsvankin, 2011, 2012; Behura et al., 2012; Vavryčuk, 2015; Zhubayev et al., 2016). In addition to energy absorption in attenuating media, it must be emphasized that other factors such as geometric spreading, reflection and transmission, and scattering by small-scale heterogeneities can also induce wave-amplitude attenuation.

Although the complex eikonal equation is formally similar to the real eikonal equation, it is very difficult to find the exact solution to the complex eikonal equation for realistic attenuating models. The complex ray-tracing method (Zhu and Chun, 1994; Thomson, 1997; Chapman et al., 1999; Kravtsov et al., 1999; Hanyga and Seredyňska, 2000; Amodei et al., 2006), which is aimed to exactly calculate the complex-valued traveltime, cannot be easily implemented in attenuating models with complicated velocity and attenuation structures because this method requires that the medium parameters defined in real space are continued to complex space, which cannot be accomplished for realistic models. For horizontally layered, attenuating media, the complex ray method may be simplified to determine the horizontal slowness component at the saddle point of the phase function of the wavefield at the receiver (Hearn and Krebes, 1990a, 1990b; Krebes and Slawinski, 1991; Le et al., 1994). On the other hand, approximate methods have been developed to solve the complex eikonal equation. These methods include real ray tracing (Vavryčuk, 2008, 2010, 2012) and real ray tracing based on model perturbation (e.g., Moczo et al., 1987; Gajewski and Pšenčík, 1992; Červený, 2001, pp. 542–548; Červený and Pšenčík, 2009; Klimeš and Klimeš, 2011).

In this paper, we propose an acoustic eikonal equation approximately governing the complex-valued traveltimes of P-waves in attenuating orthorhombic media. We extend the acoustic eikonal equation developed for attenuating transversely isotropic media with a vertical symmetry axis (VTI) by Hao and Alkhalifah (2017) to the attenuating orthorhombic case. The acoustic eikonal equation for attenuating orthorhombic media is derived by considering the acoustic assumption that the S-wave velocity parameter v_{S0} in Tsvankin's (1997) barely affects the P-wave velocity in an elastic orthorhombic medium (Alkhalifah, 2003) and the S-wave attenuation-coefficient parameter A_{S0} in Zhu and Tsvankin's (2007) notation barely affects the attenuation coefficient of homogeneous P-waves in an attenuating orthorhombic medium.

We present a perturbation method to approximately calculate the complex-valued traveltime from the acoustic eikonal equation for homogeneous attenuating orthorhombic media. The Shanks transform is also considered to accelerate the convergence of the traveltime series with respect to the perturbation parameters. A similar method is adopted by Hao and Alkhalifah (2017) to solve the acoustic eikonal equations for homogeneous attenuating VTI media. As mentioned by Hao and Alkhalifah (2017), numerical methods, such as finite-difference methods (e.g., Vidale, 1988, 1990; van Trier and Symes, 1991), fast-sweeping methods (e.g., Tsai et al., 2003; Zhang et al., 2006; Luo and Qian, 2012; Waheed et al., 2015), and fast-marching methods (e.g., Sethian, 1996; Sethian and Vladimirsky, 2001; Alkhalifah, 2011), can be used in calculating the traveltime only for nonattenuating media until now. We will not attempt to discuss the numerical scheme to directly solve the acoustic eikonal equation for heterogeneous attenuating orthorhombic medium in this paper. This issue will be addressed in a future paper.

The rest of this paper is organized as follows: We start with the exact eikonal equation for attenuating orthorhombic media. We then combine Tsvankin's (1997) notation and Zhu and Tsvankin's (2007) notation and consider the acoustic assumption to approximate the exact eikonal equation, from which we derive the acoustic eikonal equation for attenuating orthorhombic media. We next combine perturbation theory and the Shanks transform to derive the analytic eikonal solution for a homogeneous attenuating orthorhombic medium. For an orthorhombic layer with weak attenuation, we subsequently derive the series expansions for the real and imaginary parts of the reflection traveltime in terms of the source-receiver offset. Numerical examples are shown to verify the acoustic assumption, to investigate the accuracy of the analytic eikonal solution, to analyze the sensitivity of the real and imaginary parts of the traveltime to the perturbation parameters, and to investigate the reflection traveltime from an attenuating orthorhombic layer. We finally present the conclusions.

It is worth noting that we adopt the special notation originally used in Klimeš (2002) to denote the first-order spatial derivatives of the traveltime throughout the paper: The first-order derivatives of the traveltime with respect to the spatial coordinates x, y, and z are denoted by putting a comma followed by the considered spatial coordinate in the subscript. For example, $\tau_{,x}$ and $\tau_{0,x}$ denote the first-order partial derivatives of the traveltimes τ and τ_0 with respect to x, respectively.

THE EXACT EIKONAL EQUATION

For a generally attenuating anisotropic medium, the density-normalized complex-valued stiffness coefficients in the frequency domain are denoted by $a_{ij} = a_{ij}^R - ia_{ij}^I$ in Voigt notation, in which the minus sign corresponds to the sign in the exponential factor $\exp(-i\omega t)$ of a time-harmonic wave under consideration (Červený and Pšenčík, 2009), where ω and t denote the angular frequency and time; the matrices constructed by a_{ij}^R and a_{ij}^I are positive definite (Červený and Pšenčík, 2006); symbol "i" denotes the imaginary unit. According to the correspondence principle (Ben-Menahem and Singh, 1981, p. 875; Carcione, 2015, pp. 145–146), the attenuating anisotropic eikonal equation is similar in form to the nonattenuating anisotropic eikonal equation, except that the stiffness coefficients are replaced by the complex-valued stiffness coefficients. By referring to Červený (2001, pp. 62–64), the eikonal equation for attenuating orthorhombic media reads

$$\det\begin{pmatrix} a_{11}\tau_{,x}^2+a_{66}\tau_{,y}^2+a_{55}\tau_{,z}^2-1 & (a_{12}+a_{66})\tau_{,x}\tau_{,y} & (a_{13}+a_{55})\tau_{,x}\tau_{,z} \\ (a_{12}+a_{66})\tau_{,x}\tau_{,y} & a_{66}\tau_{,x}^2+a_{22}\tau_{,y}^2+a_{44}\tau_{,z}^2-1 & (a_{23}+a_{44})\tau_{,y}\tau_{,z} \\ (a_{13}+a_{55})\tau_{,x}\tau_{,z} & (a_{23}+a_{44})\tau_{,y}\tau_{,z} & a_{55}\tau_{,x}^2+a_{44}\tau_{,y}^2+a_{33}\tau_{,z}^2-1 \end{pmatrix}=0, \tag{1}$$

where $\tau_{,x}$, $\tau_{,y}$, and $\tau_{,z}$ denote the partial derivative of the complex-valued traveltime τ with respect to x, y, and z. The eikonal equation 1

governs the traveltime of P-, S1-, and S2-waves in an attenuating orthorhombic medium with the symmetry planes orthogonal to the Cartesian coordinate axes.

In addition to using stiffness coefficients in Voigt notation, an attenuating orthorhombic medium can also be fully described by the combination of Tsvankin's (1997) notation and Zhu and Tsvankin's (2007) notation. The density-normalized stiffness coefficients in equation 1 can be expressed in terms of the parameters in Tsvankin's (1997) notation and Zhu and Tsvankin's (2007) notation.

AN ACOUSTIC ATTENUATING EIKONAL EQUATION

The S-wave velocity parameter v_{S0} in Tsvankin's (1997) notation barely affects the P-wave velocity in elastic orthorhombic media, which is called the acoustic assumption for orthorhombic media (Alkhalifah, 2003). For attenuating orthorhombic media, the attenuation coefficient of a homogeneous plane P-wave is almost independent of the S-wave normalized attenuation coefficient A_{S0} in Zhu and Tsvankin's (2007) notation. Therefore, ignoring parameters v_{S0} and A_{S0} should have little effect on the P-wave traveltime in attenuating orthorhombic media.

By analogy with the derivation of acoustic eikonal equation for attenuating VTI media (Hao and Alkhalifah, 2017), we first express the stiffness coefficients in equation 1 using Tsvankin's (1997) and Zhu and Tsvankin's (2007) notations (see Appendix A) and then set v_{S0} equal to zero. As explained in Hao and Alkhalifah (2017), we do not need to set any assumptions on A_{S0} because the parameter A_{S0} vanishes in equation 2 when setting v_{S0} to zero. Furthermore, we use the modified Alkhalifah's (2003) notation (Hao et al., 2016) instead of Tsvankin's (1997) notation to describe the nonattenuating reference of the attenuating orthorhombic media under the acoustic assumption. As shown in Appendix A, the parameters in the modified Alkhalifah's (2003) notation include P-wave velocity v_{P0}, NMO velocities v_{n1} and v_{n2}, and three anellipticity parameters η_1, η_2, and η_3, where the subscripts 1, 2, and 3 correspond to the $[y, z]$, $[x, z]$, and $[x, y]$ symmetry planes of an orthorhombic medium. It follows that the acoustic eikonal equation for attenuating orthorhombic media is given by

$$\det\begin{pmatrix} a_{11}\tau_{,x}^2-1 & a_{12}\tau_{,x}\tau_{,y} & a_{13}\tau_{,x}\tau_{,z} \\ a_{12}\tau_{,x}\tau_{,y} & a_{22}\tau_{,y}^2-1 & a_{23}\tau_{,y}\tau_{,z} \\ a_{13}\tau_{,x}\tau_{,z} & a_{23}\tau_{,y}\tau_{,z} & a_{33}\tau_{,z}^2-1 \end{pmatrix}=0, \quad (2)$$

where a_{ij} are expressed by

$$a_{11}=v_{n2}^2(1-2ik(1+\varepsilon_{Q2}))(1+2\eta_2), \quad (3)$$

$$a_{12}=v_{n1}v_{n2}\xi(1-2ik(1+\varepsilon_{Q2})) - ik\delta_{Q3}(1+\varepsilon_{Q2})\frac{v_{n2}^3(1+2\eta_2)^2}{v_{n1}\xi}, \quad (4)$$

$$a_{13}=v_{P0}v_{n2}(1-2ik)-ik\delta_{Q2}\frac{v_{P0}^3}{v_{n2}}, \quad (5)$$

$$a_{22}=v_{n1}^2(1-2ik(1+\varepsilon_{Q1}))(1+2\eta_1), \quad (6)$$

$$a_{23}=v_{P0}v_{n1}(1-2ik)-ik\delta_{Q1}\frac{v_{P0}^3}{v_{n1}}, \quad (7)$$

$$a_{33}=v_{P0}^2(1-2ik), \quad (8)$$

with

$$k=\frac{A_{P0}}{1-A_{P0}^2}, \xi=\sqrt{\frac{(1+2\eta_1)(1+2\eta_2)}{1+2\eta_3}}. \quad (9)$$

Equation 2 has the similar form as the nonattenuating orthorhombic eikonal equation. Setting A_{P0} equal to zero, equation 2 reduces to the acoustic nonattenuating orthorhombic eikonal equation shown in Stovas et al. (2016).

Setting $\tau_{,y}$ equal to zero, the eikonal equation 2 reduces to the 2D acoustic eikonal equation for an attenuating VTI medium

$$A\tau_{,x}^2+B\tau_{,z}^2+C\tau_{,x}^2\tau_{,z}^2=1, \quad (10)$$

with

$$A=v_n^2(1-2ik(1+\varepsilon_Q))(1+2\eta), \quad (11)$$

$$B=v_{P0}^2(1-2ik), \quad (12)$$

$$C=\frac{v_{P0}^2}{v_n^2}((1-2ik)v_n^2-ik\delta_Q v_{P0}^2)^2 - v_{P0}^2v_n^2(1-2ik)(1-2ik(1+\varepsilon_Q))(1+2\eta), \quad (13)$$

where v_n denotes the NMO velocity, η denotes the anellipticity parameter, and ε_Q and δ_Q are the attenuation-anisotropy parameters. Equation 10 is originally presented in Hao and Alkhalifah (2017).

AN APPROXIMATE SOLUTION TO THE ACOUSTIC EIKONAL EQUATION

Let us now derive the analytic solution to the acoustic eikonal equation for homogeneous attenuating orthorhombic media. A perturbation method is adopted to solve this eikonal equation. For the nonattenuating orthorhombic eikonal equation, similar methods can be found in Masmoudi and Alkhalifah (2016) and Stovas et al. (2016). We define the vector of the perturbation parameters, $\ell=(\eta_1,\eta_2,\eta_3,\varepsilon_{Q1},\delta_{Q1},\varepsilon_{Q2},\delta_{Q2},\delta_{Q3})^T$, to represent the trial solution to equation 2:

$$\tau=\tau_0+\sum_{i=1}^{8}\tau_i\ell_i+\sum_{i,j=1;i\le j}^{8}\tau_{ij}\ell_i\ell_j, \quad (14)$$

where τ_0, τ_i, and τ_{ij} denote the zero-, first- and second-order traveltime coefficients, respectively.

Equation 14 describes the second-order approximation for the complex-valued traveltime in terms of the anellipticity parameters

and the Thomsen-type attenuation anisotropy parameters because they are considered to be independent parameters and are relatively small. It is predictable that equation 14 will become less accurate if the perturbation parameters are relatively large.

Substitution of equation 14 into the Taylor series expansions equation 2 with respect to the perturbation parameters leads to the governing equations for the zero-, first-, and second-order coefficients. The derivation of the governing equations is shown in Appendix B. These governing equations are as follows:

- The equation for the zero-order traveltime coefficient τ_0 is

$$v_{n2}^2\tau_{0,x}^2 + v_{n1}^2\tau_{0,y}^2 + v_{\mathrm{P}0}^2\tau_{0,z}^2 = \frac{1}{1-2ik}. \tag{15}$$

- The equation for the first-order traveltime coefficients τ_i is

$$v_{n2}^2\tau_{0,x}\tau_{i,x} + v_{n1}^2\tau_{0,y}\tau_{i,y} + v_{\mathrm{P}0}^2\tau_{0,z}\tau_{i,z} = f_i(\tau_0),$$
$$i = 1, 2, 3, \ldots, 8. \tag{16}$$

- The equation for the second order traveltime coefficients τ_{ij} is

$$v_{n2}^2\tau_{0,x}\tau_{ij,x} + v_{n1}^2\tau_{0,y}\tau_{ij,y} + v_{\mathrm{P}0}^2\tau_{0,z}\tau_{ij,z} = f_{ij}(\tau_0, \tau_i, \tau_j),$$
$$i, j = 1, 2, 3, \ldots, 8 \text{ and } i \le j. \tag{17}$$

The right sides of equations 16 and 17 are shown in Appendix B. The zero-, first-, and second-order traveltime coefficients can be successively calculated from equations 15 to 17. Equation 15 denotes the acoustic eikonal equation for attenuating elliptically anisotropic media. Once the zero-order traveltime is calculated from equation 15, equations 16 and 17 may be successively solved because they are the first-order linear partial differential equations. The explicit expressions for the zero-, first-, and second-order traveltime coefficients are shown in Appendix C. As a result, we may calculate the complex-valued traveltime from equation 14. The accuracy of the traveltime equation 14 is improved using the Shanks transform (Bender and Orszag, 1978, pp. 369–375):

$$\tau = T_0 + \frac{T_1^2}{T_1 - T_2}, \tag{18}$$

with

$$T_0 = \tau_0, T_1 = \sum_{i=1}^{8}\tau_i\ell_i, \qquad T_2 = \sum_{i,j=1;i\le j}^{8}\tau_{ij}\ell_i\ell_j. \tag{19}$$

Complex-valued traveltime for a horizontal, attenuating orthorhombic layer

We consider a horizontal orthorhombic layer with weak attenuation. From the approximate one-way complex-valued traveltime solution 18, we expand the reflection traveltime with respect to the normalized attenuation coefficient $A_{\mathrm{P}0}$ of Zhu and Tsvankin's (2007) notation up to first order, and with respect to the radial source-receiver offset up to fourth order. This operation may allow us to separately approximate the real and imaginary parts of the complex-valued reflection traveltime. The fourth-order series expansion for the real part of the complex-valued traveltime is given by

$$t_R^2(r,\alpha) \approx t_0^2 + \frac{r^2}{v_n^2(\alpha)} - \frac{2\eta(\alpha)r^4}{t_0^2 v_n^4(\alpha)}, \tag{20}$$

with

$$\frac{1}{v_n^2(\alpha)} = \frac{\sin^2\alpha}{v_{n1}^2} + \frac{\cos^2\alpha}{v_{n2}^2}, \tag{21}$$

$$\eta(\alpha) = \left(\frac{\sin^2\alpha}{v_{n1}^2} + \frac{\cos^2\alpha}{v_{n2}^2}\right)^{-2} \times \left(\frac{\eta_1\sin^4\alpha}{v_{n1}^4} + \frac{\eta_2\cos^4\alpha}{v_{n2}^4} + \frac{\tilde{\eta}\sin^2\alpha\cos^2\alpha}{v_{n1}^2 v_{n2}^2}\right), \tag{22}$$

where t_R denotes the real part of the complex-valued reflection traveltime; t_0 denotes the two-way zero-offset reflection traveltime in the nonattenuating reference medium corresponding to $A_{\mathrm{P}0} = 0$; r denotes the source-receiver radial offset; α denotes the acquisition azimuth measured from x-axis in the $[x, y]$ plane; the expression for $\tilde{\eta}$ is given by

$$\tilde{\eta} = -\frac{1}{2}\eta_1^2 + \eta_1(1 + \eta_2 - \eta_3) - \frac{1}{2}(\eta_2 - \eta_3)(-2 + \eta_2 + 3\eta_3)\eta_3 \approx \xi - 1, \tag{23}$$

where ξ is given in equation 9, and $\xi - 1$ is identical to the parameter η_{xy} defined in Stovas (2015).

The fourth-order series expansion for the imaginary part of complex-valued reflection traveltime is given by

$$t_I^2(r,\alpha) \approx A_{\mathrm{P}0}^2\left(t_0^2 + \frac{r^2}{v_Q^2(\alpha)} - \frac{2\eta_Q(\alpha)r^4}{t_0^2 v_Q^4(\alpha)}\right), \tag{24}$$

where t_I denotes the imaginary part of the complex-valued traveltime, the attenuation NMO velocity and anellipticity $v_Q(\alpha)$ and $\eta_Q(\alpha)$ are the functions of the acquisition azimuth α, which are defined by analogy with azimuthal NMO velocity 21 and anellipticity 22

$$\frac{1}{v_Q^2(\alpha)} = \frac{\sin^2\alpha}{v_{Q1}^2} + \frac{\cos^2\alpha}{v_{Q2}^2}, \tag{25}$$

$$\eta_Q(\alpha) = \left(\frac{\sin^2\alpha}{v_{Q1}^2} + \frac{\cos^2\alpha}{v_{Q2}^2}\right)^{-2} \times \left(\frac{\eta_{Q1}\sin^4\alpha}{v_{Q1}^4} + \frac{\eta_{Q2}\cos^4\alpha}{v_{Q2}^4} + \frac{\tilde{\eta}_Q\sin^2\alpha\cos^2\alpha}{v_{Q1}^2 v_{Q2}^2}\right), \tag{26}$$

with

$$v_{Q1} = \frac{v_{\mathrm{P}0}(1+2\delta_1)}{\sqrt{1+2\delta_1+2\delta_{Q1}}} \quad \text{and} \quad v_{Q2} = \frac{v_{\mathrm{P}0}(1+2\delta_2)}{\sqrt{1+2\delta_2+2\delta_{Q2}}}, \tag{27}$$

$$\eta_{Q1}=-\frac{\delta_{Q1}^2-2(1+2\delta_1)\delta_{Q1}(1+6\eta_1)+2(1+2\delta_1)^2(\varepsilon_{Q1}-\eta_1+2\varepsilon_{Q1}\eta_1)}{2(1+2\delta_1+2\delta_{Q1})^2}, \tag{28}$$

$$\eta_{Q2}=-\frac{\delta_{Q2}^2-2(1+2\delta_2)\delta_{Q2}(1+6\eta_2)+2(1+2\delta_2)^2(\varepsilon_{Q2}-\eta_2+2\varepsilon_{Q2}\eta_2)}{2(1+2\delta_2+2\delta_{Q2})^2}, \tag{29}$$

$$\begin{aligned}\tilde{\eta}_Q=&-\frac{1}{2(1+2\delta_1+2\delta_{Q1})(1+2\delta_2+2\delta_{Q2})}(2\delta_{Q1}\delta_{Q2}\\&-2(1+3\eta_1+3\eta_2-3\eta_3)((1+2\delta_1)\delta_{Q2}+(1+2\delta_2)\delta_{Q1})\\&+(1+2\delta_2)(2(1+2\delta_2)\delta_{Q3}(1-\eta_1+3\eta_2+\eta_3+\varepsilon_{Q2})\\&+(1+2\delta_1)(\eta_1^2-2\eta_1(1+\eta_2-\eta_3)+4\varepsilon_{Q2}(1+\eta_1+\eta_2-\eta_3)\\&+(\eta_2-\eta_3)(-2+\eta_2+3\eta_3)))),\end{aligned} \tag{30}$$

where δ_1 and δ_2 are the Thomsen-type anisotropy parameters defined in Appendix A.

Equation 30 shows that $\tilde{\eta}_Q$ is independent of attenuation-anisotropy parameter ε_{Q1}. A similar phenomenon is also found in the expression for $\varepsilon_Q(\phi)$ in equation 24 of Zhu and Tsvankin (2007). For the orthorhombic media with isotropic attenuation coefficients ($\varepsilon_{Q1}=\varepsilon_{Q2}=\delta_{Q1}=\delta_{Q2}=\delta_{Q3}=0$), the attenuation NMO velocity and attenuation anellipticity in equations 25 and 26 reduce to the NMO velocity and anellipticity in equations 21 and 22. In this case, the approximation for the imaginary part of traveltime is expressed by

$$t_I(r,\alpha)\approx A_{\mathrm{P0}}t_R(r,\alpha), \tag{31}$$

where t_R is given in equation 20.

NUMERICAL EXAMPLES

For a homogeneous attenuating medium, the complex-valued traveltime of a propagating ray is directly controlled by the ray velocity and the ray attenuation (Vavryčuk, 2007). In the first example, we investigate the influence of the S-wave parameters v_{S0} and A_{S0} on the P-wave ray velocity and ray attenuation for an attenuating orthorhombic medium. The ray velocity V_{ray} and the ray-attenuation coefficient A_{ray} are defined by Vavryčuk (2007) as follows:

$$V_{\mathrm{ray}}=\frac{v_R^2+v_I^2}{v_R}, \tag{32}$$

$$A_{\mathrm{ray}}=-\frac{2v_I}{v_R^2+v_I^2}, \tag{33}$$

where v_R and v_I denote the magnitudes of the real and imaginary parts of the complex energy-velocity vector. For a ray propagating in a homogeneous attenuating medium, the complex energy-velocity vector is homogeneous, which means that the direction of the vector constructed by the real part of the complex vector coincides with the direction of the vector constructed by the imaginary part of the complex vector. For a general attenuating anisotropic medium, Vavryčuk (2007) proposes a method to calculate the exact complex-valued energy velocity from the ray-propagation direction. In his method, a system of nonlinear polynomial equations in the un-

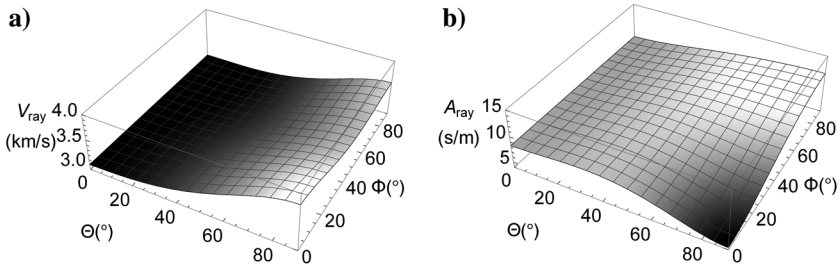

Figure 1. The (a) velocity V_{ray} and (b) attenuation A_{ray} of P-wave rays in the attenuating orthorhombic model shown in Table 1. The Θ and Φ denote the polar and azimuthal angles of the ray-propagation direction, in which the polar angle is measured from the z-axis and the azimuthal angle is measured from the x-axis in the $[x, y]$ plane. For this model, the anisotropy strengths of the velocity and attenuation of P-wave rays are approximately 0.21 and 0.89, respectively, where the anisotropy strength is defined as the absolute value of the fractional difference between the largest and smallest values of the considered quantity along all propagation directions.

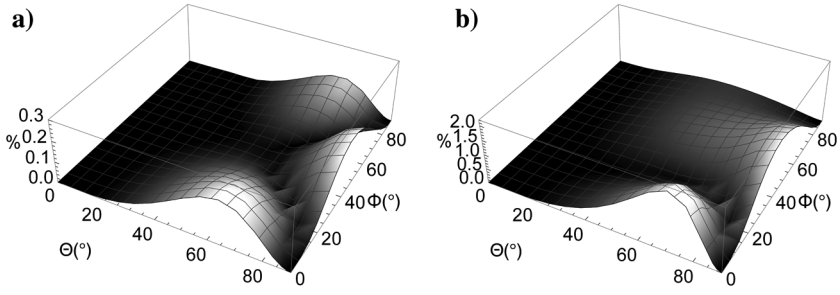

Figure 2. The relative differences in (a) velocity and (b) attenuation of P-wave rays, between the attenuating orthorhombic model and its acoustic version. The relative difference is defined as $|X-Y|/X\times 100\%$, where X and Y denote the quantities corresponding to the attenuating orthorhombic model and its acoustic version, respectively. The attenuating orthorhombic model and its acoustic version are shown in Tables 1 and 2, respectively.

Table 1. The attenuating orthorhombic model. The values of A_{P0} and A_{S0} correspond to the quality factors $Q_{33}=20$ and $Q_{55}=15$ of the vertically propagating P- and S-waves, respectively. The values of the attenuation parameters in this model are designed by referring to Zhu and Tsvankin (2007).

v_{P0}(km/s)	v_{S0}(km/s)	ε_1	δ_1	γ_1	ε_2	δ_2	γ_2	δ_3
3.0	1.5	0.2	−0.05	0.1	0.3	0.1	0.3	−0.2
A_{P0}	A_{S0}	ε_{Q1}	δ_{Q1}	γ_{Q1}	ε_{Q2}	δ_{Q2}	γ_{Q2}	δ_{Q3}
0.02498	0.03330	0.66	0.52	−0.4	−0.33	0.98	0.4	0.94

Table 2. The acoustic attenuating orthorhombic model converted from the model shown in Table 1.

v_{P0}(km/s)	v_{n1}(km/s)	v_{n2}(km/s)	η_1	η_2	η_3
3.0	2.846	3.286	0.278	0.167	0.229
A_{P0}	ε_{Q1}	δ_{Q1}	ε_{Q2}	δ_{Q2}	δ_{Q3}
0.02498	0.66	0.52	−0.33	0.98	0.94

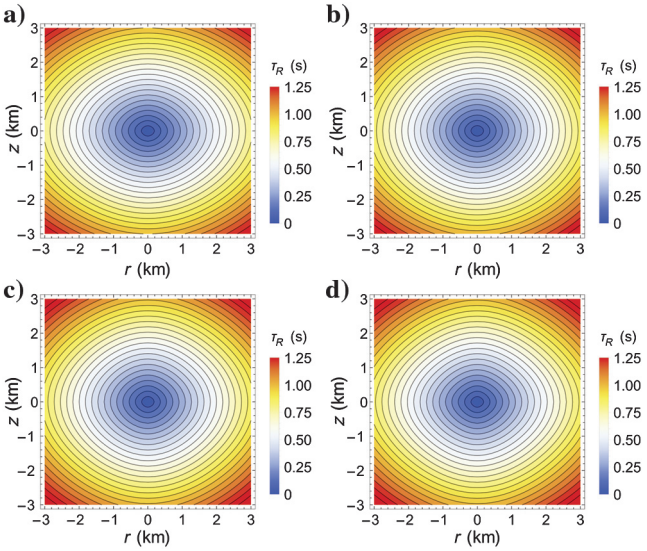

Figure 3. The real part of the exact complex-valued traveltime for a homogeneous, acoustic attenuating orthorhombic model. The r and z denote the radial and vertical coordinates, respectively. Panels (a-d) correspond to the observation azimuths 0, $\pi/6$, $\pi/3$, and $\pi/2$, respectively. The model parameters are shown in Table 2.

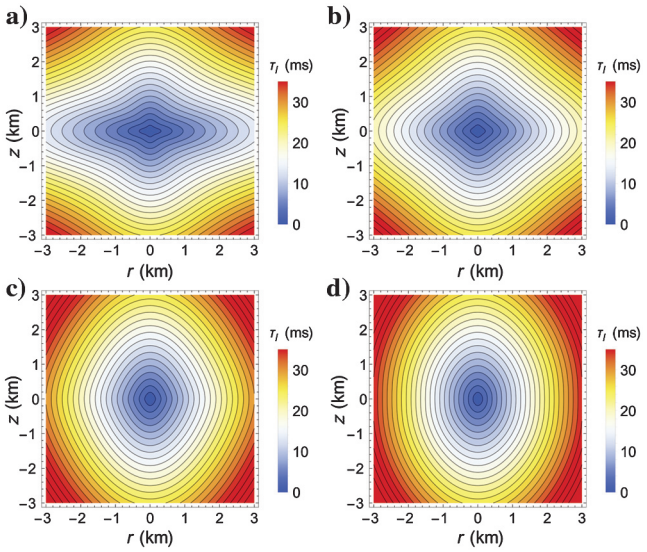

Figure 4. Similar to Figure 3, but for the imaginary parts of the exact complex-valued traveltime.

known vector of phase slowness (Vavryčuk, 2006) is numerically solved for a given ray-propagation direction. The complex-valued energy velocity is then calculated from an exact and analytic formula in terms of the vector of phase slowness (Vavryčuk, 2007). Here, we adopt Vavryčuk's (2007) method to calculate the exact ray velocity and ray attenuation.

As a reference, Figure 1 shows the velocity and the attenuation coefficient of P-wave rays in an attenuating orthorhombic model with strong velocity and attenuation anisotropy. Figure 2 shows the relative differences in the velocity and the attenuation coefficient from the attenuating orthorhombic media and the corresponding acoustic attenuating media are less than 0.3% and 2.0%,

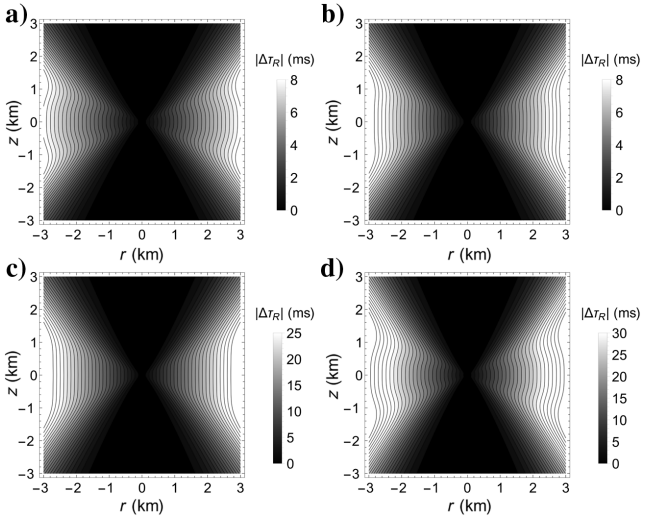

Figure 5. Absolute errors in the real part of the complex-valued traveltime from equation 14 for a homogeneous, attenuating orthorhombic medium. Panels (a-d) correspond to the observation azimuths varying from 0 to $\pi/2$ and with an interval of $\pi/6$. The model parameters are shown in Table 2.

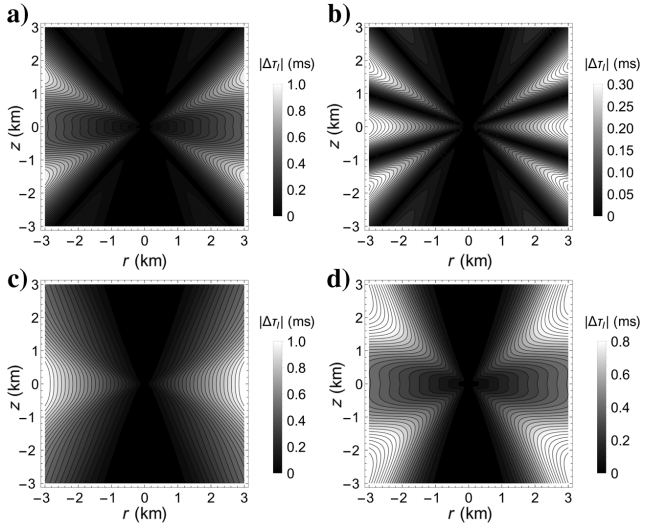

Figure 6. Similar to Figure 5, but for the imaginary part of the complex-valued traveltime.

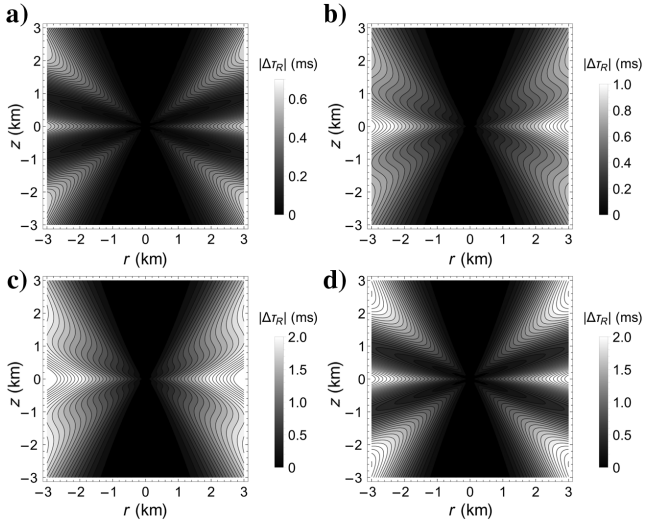

Figure 7. Absolute errors in the real part of the complex-valued traveltime from equation 18 for a homogeneous, attenuating orthorhombic medium. Panels (a-d) correspond to the observation azimuths varying from 0 to $\pi/2$ and with an interval of $\pi/6$. The model parameters are shown in Table 2.

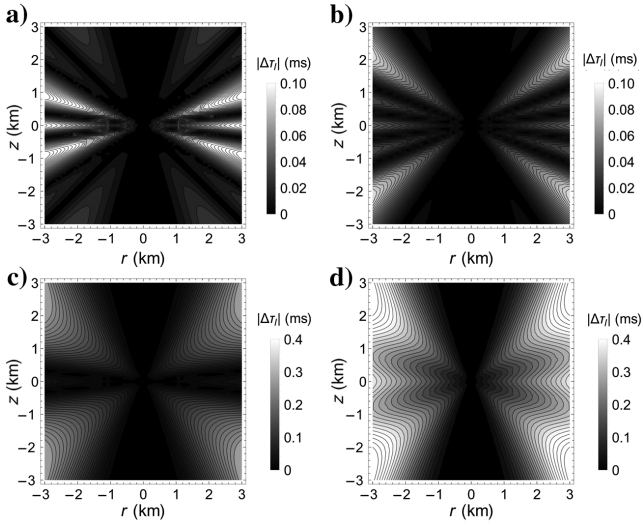

Figure 8. Similar to Figure 7, but for the imaginary part of the complex-valued traveltime.

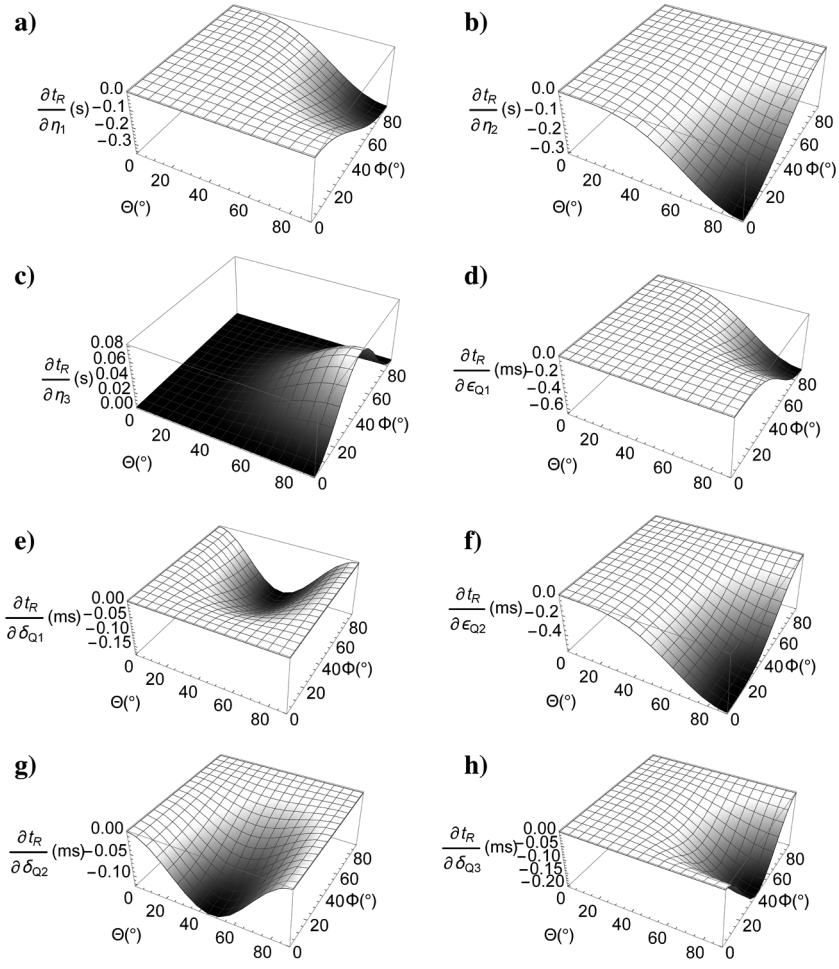

Figure 9. The first-order partial derivatives of the real part of traveltime with respect to the perturbation parameters (a) η_1, (b) η_2, (c) η_3, (d) ε_{Q1}, (e) δ_{Q1}, (f) ε_{Q2}, (g) δ_{Q2}, and (h) δ_{Q3}. The traveltime denotes the source-receiver traveltime, in which the source and receiver are located at the center and surface of a unit sphere, respectively. The Θ and Φ denote the polar and azimuthal angles of the distance vector from source to receiver, where the polar angle is measured from the z-axis and the azimuthal angle is measured from the x-axis in the $[x, y]$ plane. The model parameters are shown in Table 2.

respectively. The influence of the parameters v_{S0} and A_{S0} on the P-wave ray-attenuation coefficient is larger than their influence on the P-wave ray velocity. This example implies that the parameters v_{S0} and A_{S0} have a minor effect on the P-wave complex-valued traveltime even for an orthorhombic medium with strong velocity and attenuation anisotropy. Because the parameters v_{S0} and A_{S0} do not affect the velocity and the attenuation coefficient of P-wave rays in an attenuating isotropic medium, it is reasonable to believe that their influence on the velocity and the attenuation coefficient of P-wave rays in an attenuating orthorhombic medium is generally weak and becomes weaker with a decrease in the velocity and attenuation anisotropy.

In the second example, we compare the accuracy of the two proposed solutions 14 and 18 for a homogeneous attenuating orthorhombic model. The exact complex-valued traveltime equals to the propagation distance divided by the homogeneous complex energy velocity (Vavryčuk, 2007), in which the complex energy velocity is calculated by numerical methods in the first example. Figures 3 and 4 show the real and imaginary parts of the exact complex-valued traveltime along different acquisition azimuths. The attenuation anisotropy (corresponding to the anisotropy of the imaginary part of the complex-valued traveltime) is much stronger than the wavefront anisotropy (corresponding to the anisotropy of the real part of the complex-valued traveltime). Comparison of Figures 5 and 6 with Figures 7 and 8 shows that equation 18 is more accurate than equation 14, which implies that the Shanks transform improves the accuracy of the complex-valued perturbation expansion.

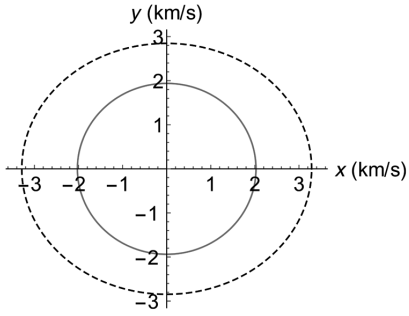

Figure 11. The azimuthal variation of NMO velocities in a horizontal, attenuating orthorhombic layer. The dashed line and the solid line denote the NMO velocity from equation 21, and the attenuation NMO velocity from equation 25, respectively. The model parameters are shown in Table 2.

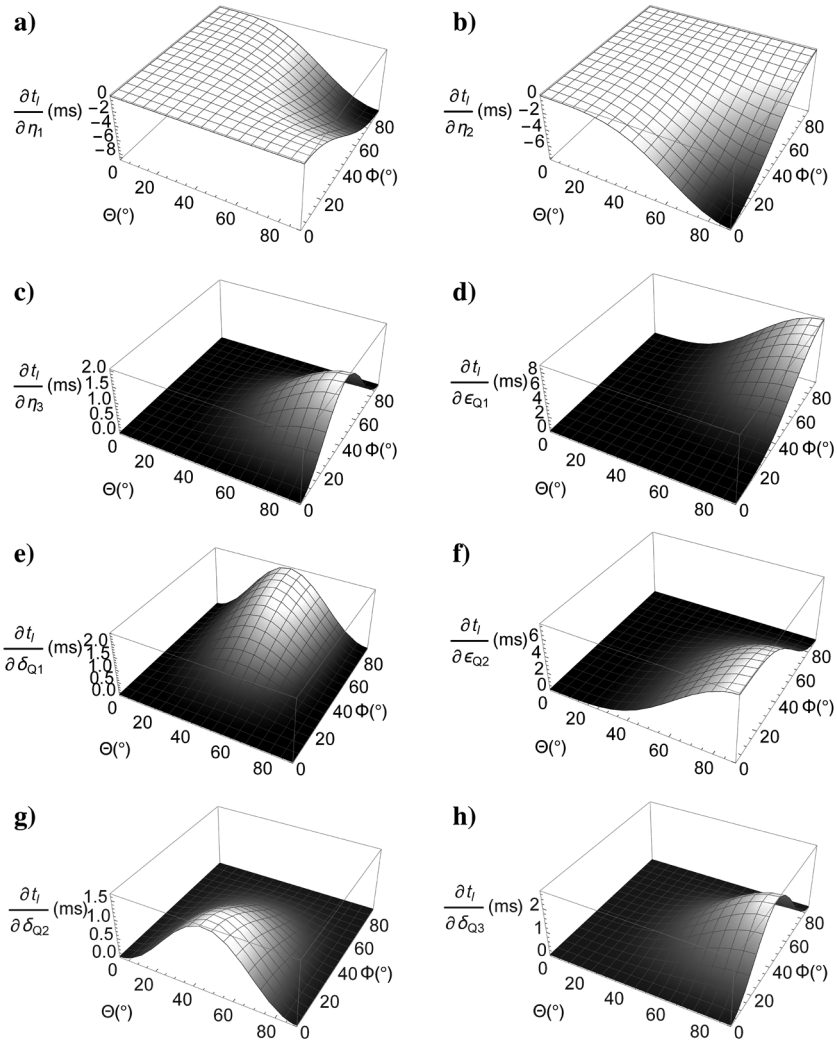

Figure 10. Similar to Figure 9, but for the imaginary part of the traveltime.

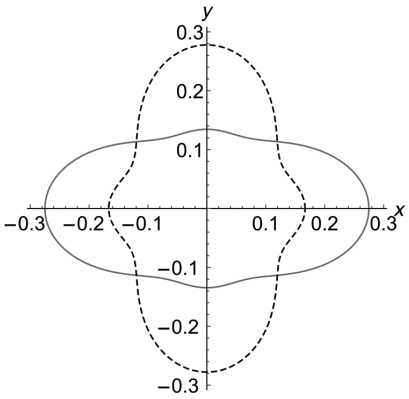

Figure 12. The azimuthal variation of anellipticities in a horizontal, attenuating orthorhombic layer. The dashed line and the solid line denote the anellipticity from equation 22, and the attenuation anellipticity from equation 26, respectively. The model parameters are shown in Table 2.

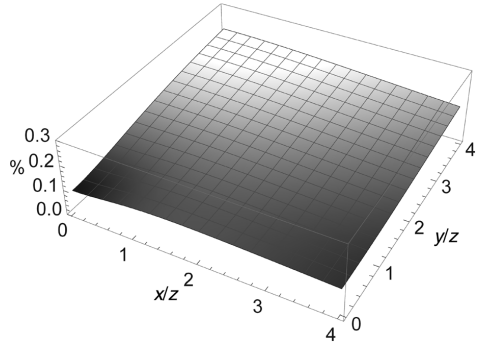

Figure 13. The relative difference between the real part of the complex-valued reflection traveltime from an attenuating orthorhombic layer and the reflection traveltime from its nonattenuating reference, in which the nonattenuating reference corresponds to the real part of the stiffness coefficient matrix of the attenuating medium. The relative difference is defined as $|t_R - t_E|/t_R \times 100\%$, where t_R and t_E denote the real part of the complex-valued traveltime from the attenuating orthorhombic model and the traveltime from its nonattenuating reference, respectively. The medium parameters of the layer are shown in Table 2. The layer thickness z is 1 km.

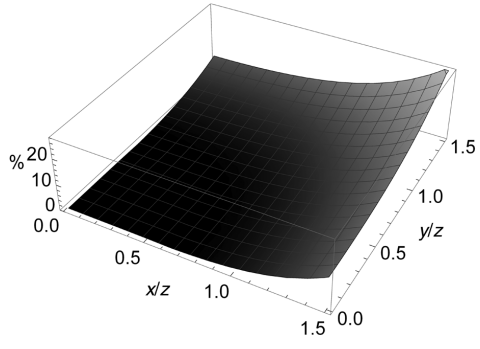

Figure 14. The relative error of the series expansion 24 for the imaginary part of traveltime of P-waves in an attenuating orthorhombic layer. The medium parameters of the layer are shown in Table 2. The layer depth is 1 km.

In the third example, we analyze the sensitivity of the real and imaginary parts of the traveltime to the anellipticity parameters (η_1, η_2, and η_3) and the attenuation-anisotropy parameters (ε_{Q1}, δ_{Q1}, ε_{Q2}, δ_{Q2}, and δ_{Q3}). The first-order partial derivatives of traveltime with respect to the considered parameters describe the sensitivity of the traveltime to these parameters. We observe the directional variation of the partial derivatives of the traveltime with respect to the considered parameters. The source and the receiver are located at the center and the surface of a unit sphere, respectively. Figure 9 shows that the real part of the traveltime is sensitive to only the anellipticity parameters. Parameters η_1 and η_2 affect the real part of the traveltime of the rays close to the $[y, z]$ and $[x, y]$ planes, respectively. Parameter η_3 affects the real part of traveltime of the rays between the $[y, z]$ and $[x, y]$ planes. Meanwhile, the influence of these anellipticity parameters on the real part of the traveltime becomes substantial only when the polar angle of the ray direction is approximately larger than 40°. The real part of the traveltime is insensitive to all the attenuation-anisotropy parameters. This implies that it could be impossible to invert for these attenuation-anisotropy parameters from the real part of the traveltime in practice. Figure 10 shows that the imaginary part of the traveltime is sensitive to all the anellipticity and attenuation-anisotropy parameters. Parameters η_1, ε_1, and δ_1 affect the imaginary part of traveltime of rays close to the $[y, z]$ planes. In contrast, parameters η_2, ε_2, and δ_2 affect the imaginary part of traveltime of rays close to the $[x, y]$ plane. Parameters η_3 and δ_3 affect the imaginary part of traveltime of rays between the $[y, z]$ and $[x, y]$ planes, and this influence becomes substantial when the polar angle of these rays is larger than 50°.

In the last example, we investigate the reflection traveltime from a horizontal, attenuating orthorhombic layer. Figure 11 shows that the attenuation NMO velocity is smaller than the NMO velocity, but the attenuation NMO velocity ellipse has a similar shape to the NMO velocity ellipse. The anellipticity affects the nonhyperbolic strength of the real part of the complex-valued reflection traveltime: the larger the anellipticity, the stronger the nonhyperbolic behavior. Similarly, the attenuation anellipticity affects the nonhyperbolic strength of the imaginary part of the complex-valued reflection traveltime. Figure 12 shows that the nonhyperbolic strength of the imaginary part of the complex-valued reflection traveltime along the x-axis is stronger than along the y-axis, whereas the nonhyperbolic strength of the real part of the complex-valued traveltime along the x-axis is weaker than along the y-axis. Figure 13 shows that the real part of the reflection traveltime from the attenuating orthorhombic layer is much closer to the reflection traveltime from its nonattenuating reference. This indicates that we can use the existing traveltime formulas developed for nonattenuating orthorhombic layers to approximately describe the real part of the complex-valued reflection traveltime from the attenuating orthorhombic layers. Figure 14 shows that the series expansion 24 for the imaginary part of the complex-valued reflection traveltime is accurate only for the ratios between the source-receiver radial offset and the layer depth is less than 0.9. The error of the series expansion increases rapidly for a larger source-receiver radial offset.

CONCLUSION

The presented acoustic eikonal equation governs the complex-valued traveltime of P-waves in attenuating orthorhombic media. This eikonal equation is derived under the assumption that the S-wave velocity parameter v_{S0} in Tsvankin's notation and the S-wave normalized attenuation coefficient A_{S0} in Zhu and Tsvankin's notation

barely affect the complex-valued traveltime of P-waves in attenuating orthorhombic media. Compared with the exact P-wave eikonal equation, the acoustic eikonal equation includes fewer parameters, which is closer to what we can practically estimate using P-wave data. The combination of a perturbation method and the Shanks transform leads to an accurate solution to the acoustic eikonal equation for homogeneous attenuating orthorhombic media.

For a homogeneous attenuating orthorhombic medium, there exists a directional dependency of the sensitivity of the real and imaginary parts of traveltime to the anellipticity parameters in the modified Alkhalifah's notation and the attenuation-anisotropy parameters in Zhu and Tsvankin's notation. Overall, the real part of the complex-valued traveltime is sensitive only to the anellipticity parameters. However, the imaginary part of the complex-valued traveltime is sensitive to not only the attenuation-anisotropy parameters but also the anellipticity parameters.

For a horizontally homogeneous orthorhombic layer with weak attenuation, the real and imaginary parts of the complex-valued reflection traveltime curves along an acquisition azimuth include the nonzero fourth-order terms, which implies that the curves for the real and imaginary parts have nonhyperbolic shapes; the real part of the complex-valued P-wave reflection traveltime is approximately independent of the attenuation parameters in Zhu and Tsvankin's notation, and it may be approximately described by the existing approximations developed for a nonattenuating orthorhombic medium; the imaginary part of the complex-valued P-wave reflection traveltime may be approximated by analogy with the traveltime approximations developed for a nonattenuating orthorhombic medium. Similar to the roles of NMO velocity and anellipticity, the attenuation NMO velocity controls the curvature of the imaginary part of the complex-valued traveltime around the zero source-receiver offset, whereas the attenuation anellipticity controls the nonhyperbolic strength of the imaginary part of the complex-valued traveltime. The real part of the complex-valued reflection traveltime can be approximately described by the existing traveltime formulas developed for the nonattenuating medium. The series expansion for the imaginary part of the complex-valued reflection traveltime is valid only for short source-receiver offsets. The accurate approximations need to be developed to describe the imaginary part of the complex-valued reflection traveltime for larger source-receiver offsets.

ACKNOWLEDGMENTS

Q. Hao thanks the rock and seismic (ROSE) project for its support and I. Pšenčík for the valuable communication on seismic wave attenuation after the 17th International Workshop on Seismic Anisotropy held in Austin. T. Alkhalifah thanks KAUST for its support. We thank the associate editor I. Ravve, Y. Sripanich, and two anonymous reviewers for their critical reviews of the manuscript.

APPENDIX A

THOMSEN-TYPE NOTATION FOR ATTENUATING ORTHORHOMBIC MEDIA

In this appendix, we show the parameterization for an attenuating orthorhombic medium with three symmetry planes orthogonal to the Cartesian coordinate axes. The frequency-domain complex-valued stiffness coefficients for an attenuating orthorhombic medium are denoted by $c_{ij} = c_{ij}^R - ic_{ij}^I$, where i denotes the imaginary unit, the minus sign corresponds to the sign in the exponential factor $\exp(-i\omega t)$ of a time-harmonic wave under consideration (Červený and Pšenčík, 2009), where ω and t denote the angular frequency and time. For a time-harmonic plane wave with the exponential factor $\exp(-i\omega t)$, the time-average strain energy and the dissipated energy are positive in an attenuating anisotropic medium. This requires that matrices composed of c_{ij}^R and c_{ij}^I are positive definite (Červený and Pšenčík, 2006). The Q-matrix is defined by $Q_{ij} \equiv c_{ij}^R/c_{ij}^I$ corresponding to the stiffness coefficients $c_{ij} = c_{ij}^R - ic_{ij}^I$ and traveltime $\tau = \tau_R + i\tau_I$. The density of the medium is denoted by ρ. Tsvankin's (1997) and Zhu and Tsvankin's (2007) notations are combined to parameterize an attenuating orthorhombic medium. Tsvankin's (1997) notation is used to describe the wave velocities in the elastic reference corresponding to the real part of the stiffness coefficients of an attenuating orthorhombic medium. Zhu and Tsvankin's (2007) notation is used to describe the attenuation coefficients of homogeneous plane waves in an attenuating orthorhombic medium. An attenuating orthorhombic medium is parameterized by the following parameters:

- v_{P0}: the velocity of the vertically propagating P-waves

$$v_{P0} \equiv \sqrt{\frac{c_{33}^R}{\rho}}. \tag{A-1}$$

- v_{S0}: the velocity of the vertically propagating S-waves polarized along the x-axis

$$v_{S0} \equiv \sqrt{\frac{c_{55}^R}{\rho}}. \tag{A-2}$$

- $\varepsilon_1, \delta_1, \gamma_1$: the Thomsen-type parameters defined in the $[y, z]$ plane (the superscript 1 corresponds to the x-axis normal to the $[y, z]$ plane)

$$\varepsilon_1 \equiv \frac{c_{22}^R - c_{33}^R}{2c_{33}^R}, \tag{A-3}$$

$$\delta_1 \equiv \frac{(c_{23}^R + c_{44}^R)^2 - (c_{33}^R - c_{44}^R)^2}{2c_{33}^R(c_{33}^R - c_{44}^R)}, \tag{A-4}$$

$$\gamma_1 \equiv \frac{c_{66}^R - c_{55}^R}{2c_{55}^R}. \tag{A-5}$$

- $\varepsilon_2, \delta_2, \gamma_2$: the Thomsen-type parameters defined in the $[x, z]$ plane (the superscript 2 corresponds to the y-axis normal to the $[x, z]$ plane)

$$\varepsilon_2 \equiv \frac{c_{11}^R - c_{33}^R}{2c_{33}^R}, \tag{A-6}$$

$$\delta_2 \equiv \frac{(c_{13}^R + c_{55}^R)^2 - (c_{33}^R - c_{55}^R)^2}{2c_{33}^R(c_{33}^R - c_{55}^R)}, \tag{A-7}$$

$$\gamma_2 \equiv \frac{c_{66}^R - c_{44}^R}{2c_{44}^R}. \tag{A-8}$$

- δ_3: the Thomsen-type parameters defined in the $[x, y]$ plane (the superscript 3 corresponds to the z-axis normal to the $[x, z]$ plane; the x-axis plays the role of the symmetry axis)

$$\delta_3 \equiv \frac{(c_{12}^R + c_{66}^R)^2 - (c_{11}^R - c_{66}^R)^2}{2c_{11}^R(c_{11}^R - c_{66}^R)}. \tag{A-9}$$

- A_{P0}: the P-wave normalized attenuation coefficient in the symmetry (vertical) direction

$$A_{P0} \equiv Q_{33}\left(\sqrt{1+\frac{1}{Q_{33}^2}}-1\right). \tag{A-10}$$

- A_{S0}: the S-wave normalized attenuation coefficient in the symmetry (vertical) direction

$$A_{S0} \equiv Q_{55}\left(\sqrt{1+\frac{1}{Q_{55}^2}}-1\right). \tag{A-11}$$

- ε_{Q1}, δ_{Q1}, γ_{Q1}: the Thomsen-type parameters for attenuation anisotropy defined in the $[y, z]$ plane

$$\varepsilon_{Q1} \equiv \frac{Q_{33} - Q_{22}}{Q_{22}}, \tag{A-12}$$

$$\delta_{Q1} \equiv \frac{\frac{Q_{33}-Q_{44}}{Q_{44}} c_{44}^R \frac{(c_{23}^R + c_{33}^R)^2}{(c_{33}^R - c_{44}^R)} + 2\frac{Q_{33}-Q_{23}}{Q_{23}} c_{23}^R (c_{23}^R + c_{44}^R)}{c_{33}^R(c_{33}^R - c_{44}^R)}, \tag{A-13}$$

$$\gamma_{Q1} \equiv \frac{Q_{55} - Q_{66}}{Q_{66}}. \tag{A-14}$$

- ε_{Q2}, δ_{Q2}, γ_{Q2}: the Thomsen-type parameters for attenuation anisotropy defined in the $[x, z]$ plane

$$\varepsilon_{Q2} \equiv \frac{Q_{33} - Q_{11}}{Q_{11}}, \tag{A-15}$$

$$\delta_{Q2} \equiv \frac{\frac{Q_{33}-Q_{55}}{Q_{55}} c_{55}^R \frac{(c_{13}^R + c_{55}^R)^2}{(c_{33}^R - c_{55}^R)} + 2\frac{Q_{33}-Q_{13}}{Q_{13}} c_{13}^R (c_{13}^R + c_{55}^R)}{c_{33}^R(c_{33}^R - c_{55}^R)}, \tag{A-16}$$

$$\gamma_{Q2} \equiv \frac{Q_{44} - Q_{66}}{Q_{66}}. \tag{A-17}$$

- δ_{Q3}: the Thomsen-type parameters for attenuation anisotropy, defined in the $[x, y]$ plane

$$\delta_{Q3} \equiv \frac{\frac{Q_{11}-Q_{66}}{Q_{66}} c_{55}^R \frac{(c_{11}^R + c_{12}^R)^2}{(c_{11}^R - c_{66}^R)} + 2\frac{Q_{11}-Q_{12}}{Q_{12}} c_{12}^R (c_{12}^R + c_{66}^R)}{c_{11}^R(c_{11}^R - c_{66}^R)}. \tag{A-18}$$

In the "An acoustic attenuating eikonal equation" section, we consider the S-wave parameter $v_{S0} = 0$ to derive the approximate eikonal equation governing P-wave traveltimes in an attenuating orthorhombic medium. As explained in that section, the S-wave parameter A_{S0} in Zhu and Tsvankin's (2007) notation will vanish from the acoustic attenuating eikonal equation. Except for v_{P0}, the other parameters in Tsvankin's (1997) notation are replaced by the modified Alkhalifah's (2003) notation (Hao et al., 2016) to describe the nonattenuation part of the P-waves in an attenuating orthorhombic medium because the parameters in the later notation are more closely linked to the P-wave anisotropy for nonattenuating orthorhombic media. In addition to the P-wave velocity v_{P0} defined in equation A-1, the other parameters in the modified Alkhalifah's notation are defined as follows:

$$v_{n1} \equiv v_{P0}\sqrt{1+2\delta_1} = \sqrt{\frac{(c_{23}^R)^2 + 2c_{23}^R c_{44}^R + c_{33}^R c_{44}^R}{\rho(c_{33}^R - c_{44}^R)}}, \tag{A-19}$$

$$v_{n2} \equiv v_{P0}\sqrt{1+2\delta_2} = \sqrt{\frac{(c_{13}^R)^2 + 2c_{13}^R c_{55}^R + c_{33}^R c_{55}^R}{\rho(c_{33}^R - c_{55}^R)}}, \tag{A-20}$$

$$\eta_1 \equiv \frac{\varepsilon_1 - \delta_1}{1+2\delta_1} = \frac{c_{22}^R(c_{33}^R - c_{44}^R)}{2((c_{23}^R)^2 + 2c_{23}^R c_{44}^R + c_{33}^R c_{44}^R)} - \frac{1}{2}, \tag{A-21}$$

$$\eta_2 \equiv \frac{\varepsilon_2 - \delta_2}{1+2\delta_2} = \frac{c_{11}^R(c_{33}^R - c_{55}^R)}{2((c_{13}^R)^2 + 2c_{13}^R c_{55}^R + c_{33}^R c_{55}^R)} - \frac{1}{2}, \tag{A-22}$$

$$\eta_3 \equiv \frac{\varepsilon_1 - \varepsilon_2 - \delta_3(1+2\varepsilon_2)}{(1+2\delta_3)(1+2\varepsilon_2)} = \frac{c_{22}^R(c_{11}^R - c_{66}^R)}{2((c_{12}^R)^2 + 2c_{12}^R c_{66}^R + c_{11}^R c_{66}^R)} - \frac{1}{2}, \tag{A-23}$$

where subscripts 1, 2, 3 except for c_{ij}^R correspond to the $[y, z]$, $[x, z]$, and $[x, y]$ symmetry planes of an orthorhombic medium, respectively; v_{ni} $(i = 1, 2)$ denote the NMO velocities; and η_i $(i = 3, 2, 3)$ denote the anellipticity parameters (Grechka and Tsvankin, 1999).

APPENDIX B

THE GOVERNING EQUATIONS FOR TRAVELTIME COEFFICIENTS

In this appendix, we derive the governing equations for traveltime coefficients as illustrated in equations 15–17.

The acoustic eikonal equation 2 is generally expressed by

$$F(\boldsymbol{\ell}, \tau_{,x}, \tau_{,y}, \tau_{,z}) = 0, \tag{B-1}$$

where function F represents the left side of equation 2; $\boldsymbol{\ell} = (\eta_1, \eta_2, \eta_3, \varepsilon_{Q1}, \delta_{Q1}, \varepsilon_{Q2}, \delta_{Q2}, \delta_{Q3})^T$ denotes the vector of perturbation parameters; $\tau_{,x}$, $\tau_{,y}$, and $\tau_{,z}$ denote the slowness components, which denote the partial derivative of traveltime τ with respect to x, y, and z. It is noted that the stiffness coefficients a_{ij} in equation 2 are explicit functions of $\boldsymbol{\ell}$.

In equation B-1, traveltime is regarded as an implicit function of perturbation parameters. Therefore, the Taylor series of equation B-1 with respect to the perturbation parameters is given by

$$F|_{\boldsymbol{\ell}=0}+\sum_{i=1}^{8}\left(\frac{\partial F}{\partial \ell_i}+\frac{\partial F}{\partial \tau_{,K}}\frac{\partial \tau_{,K}}{\partial \ell_i}\right)\Bigg|_{\boldsymbol{\ell}=0}\ell_i+\frac{1}{2}\sum_{i,j=1}^{8}\left(\frac{\partial^2 F}{\partial \ell_i\partial \ell_j}+\frac{\partial^2 F}{\partial \ell_i\partial \tau_{,K}}\frac{\partial \tau_{,K}}{\partial \ell_j}+\frac{\partial^2 F}{\partial \ell_j\partial \tau_{,K}}\frac{\partial \tau_{,K}}{\partial \ell_i}+\frac{\partial^2 F}{\partial \tau_{,K}\partial \tau_{,M}}\frac{\partial \tau_{,K}}{\partial \ell_i}\frac{\partial \tau_{,M}}{\partial \ell_j}+\frac{\partial F}{\partial \tau_{,K}}\frac{\partial^2 \tau_{,K}}{\partial \ell_i\partial \ell_j}\right)\Bigg|_{\boldsymbol{\ell}=0}\ell_i\ell_j+\cdots=0, \tag{B-2}$$

where the uppercase subscripts K and M take x, y, and z and Einstein summation convention over subscripts K and M are considered.

As illustrated in equation 14, the trial solution to equation B-1 is defined as the second-order expansion of traveltime with respect to the perturbation parameters

$$\tau=\tau_0+\sum_{i=1}^{8}\tau_i\ell_i+\sum_{i,j=1;i\le j}^{8}\tau_{ij}\ell_i\ell_j, \tag{B-3}$$

where τ_0, τ_i, and τ_{ij} are the undetermined zero-, first-, and second-order traveltime coefficients.

To determine the equations governing the traveltime coefficients, we define the following notations:

$$F_0\equiv F(\boldsymbol{\ell}=0,\tau_{0,x},\tau_{0,y},\tau_{0,z}), \tag{B-4}$$

$$F_i\equiv\frac{\partial F(\boldsymbol{\ell},\tau_{0,x},\tau_{0,y},\tau_{0,z})}{\partial \ell_i}\Bigg|_{\boldsymbol{\ell}=0},\quad i=1,2,3,\ldots,8, \tag{B-5}$$

$$F_{ij}\equiv\frac{\partial^2 F(\boldsymbol{\ell},\tau_{0,x},\tau_{0,y},\tau_{0,z})}{\partial \ell_i\partial \ell_j}\Bigg|_{\boldsymbol{\ell}=0},\quad i,j=1,2,3,\ldots,8\text{ and }i\le j. \tag{B-6}$$

Before calculating the expansion coefficients at $\boldsymbol{\ell}=0$ in equation B-2, we insert the trial solution B-3 into equation B-2, which implies that the zero-, first-, and second-order expansion coefficients in equation B-2 are zero after considering $\boldsymbol{\ell}=0$. Therefore, we may derive the following equations about the traveltime coefficients:

$$F_0=0, \tag{B-7}$$

$$F_i+\frac{\partial F_0}{\partial \tau_{0,K}}\tau_{i,K}=0,\quad i=1,2,3,\ldots,8, \tag{B-8}$$

$$F_{ij}+\frac{\partial F_i}{\partial \tau_{0,K}}\tau_{j,K}+\frac{\partial F_j}{\partial \tau_{0,K}}\tau_{j,K}+\frac{\partial^2 F_0}{\partial \tau_{0,K}\partial \tau_{0,M}}\tau_{i,K}\tau_{j,M}+(1+\delta_{ij})\frac{\partial F_0}{\partial \tau_{0,K}}\tau_{ij,K}=0,\quad i,j=1,2,3,\ldots,8\text{ and }i\le j. \tag{B-9}$$

In equation B-7, δ_{ij} is the Kronecker delta function; the expression for F_0 is obtained from equations 2–8 as well as B-1 and B-4

$$F_0=(1-2ik)(v_{n2}^2\tau_{0,x}^2+v_{n1}^2\tau_{0,y}^2+v_{\mathrm{P0}}^2\tau_{0,z}^2)-1, \tag{B-10}$$

where k is defined by the first of equation 9.

From equations B-7 and B-10, we obtain the governing equation for the zero-order traveltime coefficients

$$v_{n2}^2\tau_{0,x}^2+v_{n1}^2\tau_{0,y}^2+v_{\mathrm{P0}}^2\tau_{0,z}^2=\frac{1}{1-2ik}. \tag{B-11}$$

In a similar way, we obtain the governing equations for the first- and second-order traveltime coefficients from equations B-8 and B-9

$$v_{n2}^2\tau_{0,x}\tau_{i,x}+v_{n1}^2\tau_{0,y}\tau_{i,y}+v_{\mathrm{P0}}^2\tau_{0,z}\tau_{i,z}=f_i(\tau_0),\quad i=1,2,3,\ldots,8, \tag{B-12}$$

$$v_{n2}^2\tau_{0,x}\tau_{ij,x}+v_{n1}^2\tau_{0,y}\tau_{ij,y}+v_{\mathrm{P0}}^2\tau_{0,z}\tau_{ij,z}=f_{ij}(\tau_0,\tau_i,\tau_j),\quad i,j=1,2,3,\ldots,8\text{ and }i\le j, \tag{B-13}$$

with

$$f_i(\tau_0)=-\frac{F_i}{2(1-2ik)},\quad i=1,2,3,\ldots,8, \tag{B-14}$$

$$f_{ij}(\tau_0,\tau_i,\tau_j)=-\frac{1}{2(1+\delta_{ij})(1-2ik)}\times\left(F_{ij}+\frac{\partial F_i}{\partial \tau_{0,K}}\tau_{j,K}+\frac{\partial F_j}{\partial \tau_{0,K}}\tau_{i,K}+\frac{\partial^2 F_0}{\partial \tau_{0,K}\partial \tau_{0,M}}\tau_{i,K}\tau_{j,M}\right),\quad i,j=1,2,3,\ldots,8\text{ and }i\le j, \tag{B-15}$$

where functions F_i and F_{ij} are obtained from equations B-5 and B-6. Furthermore, we may obtain the analytic expression for $f_i(\tau_0)$ and $f_{ij}(\tau_0,\tau_i,\tau_j)$. However, the resulting algebra for $f_{ij}(\tau_0,\tau_i,\tau_j)$ is heavy. The analytic expressions for $f_i(\tau_0)$ are as follows:

$$f_1=-\frac{1}{2}v_{n1}^2\tau_{0,y}^2+(1-2ik)v_{\mathrm{P0}}^2v_{n1}^2\tau_{0,y}^2\tau_{0,z}^2, \tag{B-16}$$

$$f_2=-\frac{1}{2}v_{n2}^2\tau_{0,x}^2+(1-2ik)v_{\mathrm{P0}}^2v_{n2}^2\tau_{0,x}^2\tau_{0,z}^2, \tag{B-17}$$

$$f_3=-(1-2ik)v_{n1}^2v_{n2}^2\tau_{0,x}^2\tau_{0,y}^2, \tag{B-18}$$

$$f_4=-\frac{2ik}{(1-2ik)}v_{n1}^2\tau_{0,y}^2-ikv_{n1}^2v_{n2}^2\tau_{0,x}^2\tau_{0,y}^2-ikv_{\mathrm{P0}}^2v_{n1}^2\tau_{0,y}^2\tau_{0,z}^2, \tag{B-19}$$

$$f_5=ikv_{\mathrm{P0}}^4\tau_{0,y}^2\tau_{0,z}^2, \tag{B-20}$$

$$f_6=-\frac{2ik}{1-2ik}v_{n2}^2\tau_{0,x}^2-ikv_{n1}^2v_{n2}^2\tau_{0,x}^2\tau_{0,y}^2-ikv_{\mathrm{P0}}^2v_{n2}^2\tau_{0,x}^2\tau_{0,z}^2, \tag{B-21}$$

$$f_7 = -ik\upsilon_{P0}^4\tau_{0,x}^2\tau_{0,z}^2, \tag{B-22}$$

$$f_8 = ik\upsilon_{n2}^4\tau_{0,x}^2\tau_{0,y}^2. \tag{B-23}$$

The analytic expressions for $f_{ij}(\tau_0, \tau_i, \tau_j)$ are accessible by contacting the first author of the paper.

APPENDIX C

THE PERTURBATION COEFFICIENTS IN EQUATION 14 FOR A HOMOGENEOUS, ATTENUATING ORTHORHOMBIC MEDIUM

In this appendix, we show the zero-, first-, and second-order coefficients of equation 14 for a homogeneous, attenuating orthorhombic medium. The single source is located at the origin of the Cartesian coordinate system.

We preliminarily define the following intermediate quantities:

$$\tau_x \equiv \frac{x}{\upsilon_{n2}}, \quad \tau_y \equiv \frac{y}{\upsilon_{n2}}, \quad \tau_z \equiv \frac{z}{\upsilon_{P0}}, \tag{C-1}$$

$$\zeta \equiv \sqrt{\tau_x^2 + \tau_y^2 + \tau_z^2}, \tag{C-2}$$

$$\lambda \equiv \sqrt{1 - 2ik}. \tag{C-3}$$

The analytic expressions for the coefficients in equation 14 are given as follows:

The zero-order coefficients

$$\tau_0 = \lambda^{-1}\zeta \tag{C-4}$$

The first-order coefficients

$$\tau_1 = -\zeta^{-3}\lambda^{-1}\tau_y^2(\tau_x^2 + \tau_y^2), \tag{C-5}$$

$$\tau_2 = -\zeta^{-3}\lambda^{-1}\tau_x^2(\tau_x^2 + \tau_y^2), \tag{C-6}$$

$$\tau_3 = \zeta^{-3}\lambda^{-1}\tau_x^2\tau_y^2, \tag{C-7}$$

$$\tau_4 = i\zeta^{-3}k\lambda^{-2}\tau_y^4, \tag{C-8}$$

$$\tau_5 = ik\zeta^{-3}\upsilon_{n1}^{-2}\lambda^{-3}\upsilon_{P0}^2\tau_y^2\tau_z^2, \tag{C-9}$$

$$\tau_6 = ik\zeta^{-3}\lambda^{-3}\tau_x^2(\tau_x^2 + 2\tau_y^2), \tag{C-10}$$

$$\tau_7 = ik\zeta^{-3}\upsilon_{n2}^{-2}\upsilon_{P0}^2\tau_x^2\tau_z^2, \tag{C-11}$$

$$\tau_8 = ik\zeta^{-3}\lambda^{-3}\upsilon_{n1}^{-2}\upsilon_{n2}^2\tau_x^2\tau_y^2. \tag{C-12}$$

The second-order coefficients

$$\tau_{11} = \frac{1}{2}\zeta^{-7}\lambda^{-1}\tau_y^2((\tau_x^2 + \tau_y^2)^2(4\tau_x^2 + 3\tau_y^2) + (\tau_x^2 + \tau_y^2)(5\tau_x^2 + 12\tau_y^2)\tau_z^2 + \tau_x^2\tau_z^4), \tag{C-13}$$

$$\tau_{12} = -\zeta^{-7}\lambda^{-1}\tau_x^2\tau_y^2((\tau_x^2 + \tau_y^2)^2 - 7(\tau_x^2 + \tau_y^2)\tau_z^2 + \tau_z^4), \tag{C-14}$$

$$\tau_{13} = \zeta^{-7}\lambda^{-1}\tau_x^2\tau_y^2(-2\tau_x^4 + \tau_y^4 - 7\tau_y^2\tau_z^2 + \tau_z^4 - \tau_x^2(\tau_y^2 + \tau_z^2)), \tag{C-15}$$

$$\tau_{14} = -i\zeta^{-7}\lambda^{-3}k\tau_y^4(4\tau_x^4 + 5\tau_x^2\tau_y^2 + \tau_y^4 + 2(\tau_x^2 + 4\tau_y^2)\tau_z^2 - 2\tau_z^4), \tag{C-16}$$

$$\tau_{15} = -3ik\zeta^{-7}\upsilon_{n1}^{-2}\lambda^{-3}\upsilon_{P0}^2\tau_y^2\tau_z^2(\tau_x^4 - \tau_y^4 + (\tau_x^2 + 2\tau_y^2)\tau_z^2), \tag{C-17}$$

$$\tau_{16} = 2ik\zeta^{-7}\lambda^{-3}\tau_x^2\tau_y^2(2\tau_y^2(\tau_x^2 + \tau_y^2) - (5\tau_x^2 + 9\tau_y^2)\tau_z^2 + \tau_z^4), \tag{C-18}$$

$$\tau_{17} = 3i\zeta^{-7}\lambda^{-3}k\upsilon_{P0}^2\tau_x^2\tau_y^2\tau_z^2(2(\tau_x^2 + \tau_y^2) - \tau_z^2), \tag{C-19}$$

$$\tau_{18} = -i\zeta^{-7}\lambda^{-3}\upsilon_{n1}^{-2}k\upsilon_{n2}^2\tau_x^2\tau_y^2(4\tau_x^4 + \tau_y^4 + 11\tau_y^2\tau_z^2 + \tau_z^4 + 5\tau_x^2(\tau_y^2 + \tau_z^2)), \tag{C-20}$$

$$\tau_{22} = \frac{1}{2}\zeta^{-7}\lambda^{-1}\tau_x^2((\tau_x^2 + \tau_y^2)^2(3\tau_x^2 + 4\tau_y^2) + (\tau_x^2 + \tau_y^2)(12\tau_x^2 + 5\tau_y^2)\tau_z^2 + \tau_y^2\tau_z^4), \tag{C-21}$$

$$\tau_{23} = \zeta^{-7}\lambda^{-1}\tau_x^2\tau_y^2(\tau_x^4 - 2\tau_y^4 - \tau_y^2\tau_z^2 + \tau_z^4 - \tau_x^2(\tau_y^2 + 7\tau_z^2)), \tag{C-22}$$

$$\tau_{24} = 3i\zeta^{-7}\lambda^{-3}k\tau_x^2\tau_y^4(\tau_x^2 + \tau_y^2 - 2\tau_z^2), \tag{C-23}$$

$$\tau_{25} = 3i\zeta^{-7}\lambda^{-3}\upsilon_{n1}^{-2}k\upsilon_{P0}^2\tau_x^2\tau_y^2\tau_z^2(2(\tau_x^2 + \tau_y^2) - \tau_z^2), \tag{C-24}$$

$$\tau_{26} = -i\zeta^{-7}\lambda^{-3}k\tau_x^2(\tau_x^6 + 3\tau_x^4\tau_y^2 + 6\tau_x^2\tau_y^4 + 4\tau_y^6 + 2(4\tau_x^4 + 8\tau_x^2\tau_y^2 + \tau_y^4)\tau_z^2 - 2(\tau_x^2 + \tau_y^2)\tau_z^4), \tag{C-25}$$

$$\tau_{27} = 3i\zeta^{-7}\lambda^{-3}v_{n2}^{-2}kv_{P0}^{2}\tau_x^2\tau_z^2(\tau_x^4 - \tau_y^4 - (2\tau_x^2 + \tau_y^2)\tau_z^2), \quad \text{(C-26)}$$

$$\tau_{28} = 3i\zeta^{-7}\lambda^{-3}v_{n1}^{-2}kv_{n2}^{2}\tau_x^2\tau_y^2(\tau_x^4 + \tau_x^2(\tau_y^2 - \tau_z^2) + \tau_z^2(\tau_y^2 + \tau_z^2)), \quad \text{(C-27)}$$

$$\tau_{33} = -\frac{1}{2}3\zeta^{-7}\lambda^{-1}\tau_x^2\tau_y^2(3\tau_x^2\tau_y^2 + (\tau_x^2 + \tau_y^2)\tau_z^2 + \tau_z^4), \quad \text{(C-28)}$$

$$\tau_{34} = 3i\zeta^{-7}\lambda^{-3}k\tau_x^2\tau_y^4(2\tau_x^2 - \tau_y^2 + 2\tau_z^2), \quad \text{(C-29)}$$

$$\tau_{35} = 3i\zeta^{-7}\lambda^{-3}v_{n1}^{-2}kv_{P0}^{2}\tau_x^2\tau_y^2\tau_z^2(\tau_x^2 - 2\tau_y^2 + \tau_z^2), \quad \text{(C-30)}$$

$$\tau_{36} = i\zeta^{-7}\lambda^{-3}k\tau_x^2\tau_y^2((\tau_x^2 - 2\tau_y^2)^2 + 2(4\tau_x^2 + \tau_y^2)\tau_z^2 - 2\tau_z^4), \quad \text{(C-31)}$$

$$\tau_{37} = -3i\zeta^{-7}\lambda^{-3}v_{n2}^{-2}kv_{P0}^{2}\tau_x^2\tau_y^2\tau_z^2(2\tau_x^2 - \tau_y^2 - \tau_z^2), \quad \text{(C-32)}$$

$$\tau_{38} = ik\zeta^{-7}\lambda^{-3}v_{n1}^{-2}v_{n2}^{2}\tau_x^2\tau_y^2(4\tau_x^4 - \tau_x^2\tau_y^2 + 4\tau_y^4 + 5(\tau_x^2 + \tau_y^2)\tau_z^2 + \tau_z^4), \quad \text{(C-33)}$$

$$\tau_{44} = -\frac{1}{2}3\zeta^{-7}\lambda^{-5}k^2\tau_y^6(4\tau_x^2 + \tau_y^2 + 4\tau_z^2), \quad \text{(C-34)}$$

$$\tau_{45} = 3\zeta^{-7}\lambda^{-5}v_{n1}^{-2}k^2v_{P0}^{2}\tau_y^4\tau_z^2(-2\tau_x^2 + \tau_y^2 - 2\tau_z^2), \quad \text{(C-35)}$$

$$\tau_{46} = -3\zeta^{-7}\lambda^{-5}k^2\tau_x^2\tau_y^4(\tau_x^2 - 2\tau_y^2 + 4\tau_z^2), \quad \text{(C-36)}$$

$$\tau_{47} = 9\zeta^{-7}\lambda^{-5}v_{n2}^{-2}k^2v_{P0}^{2}\tau_x^2\tau_y^4\tau_z^2, \quad \text{(C-37)}$$

$$\tau_{48} = -3\zeta^{-7}\lambda^{-5}v_{n1}^{-2}k^2v_{n2}^{2}\tau_x^2\tau_y^4(2\tau_x^2 - \tau_y^2 + 2\tau_z^2), \quad \text{(C-38)}$$

$$\tau_{55} = -\frac{3}{2}\zeta^{-7}\lambda^{-5}v_{n1}^{-4}k^2v_{P0}^{4}\tau_y^2\tau_z^2(\tau_y^4 - \tau_y^2\tau_z^2 + \tau_z^4 + \tau_x^2(\tau_y^2 + \tau_z^2)), \quad \text{(C-39)}$$

$$\tau_{56} = 3\zeta^{-7}\lambda^{-5}v_{n1}^{-2}k^2v_{P0}^{2}\tau_x^2\tau_y^2\tau_z^2(\tau_x^2 + 4\tau_y^2 - 2\tau_z^2), \quad \text{(C-40)}$$

$$\tau_{57} = -3\zeta^{-7}\lambda^{-5}v_{n1}^{-2}v_{n2}^{-2}k^2v_{P0}^{4}\tau_x^2\tau_y^2\tau_z^2(\tau_x^2 + \tau_y^2 - 2\tau_z^2), \quad \text{(C-41)}$$

$$\tau_{58} = -3\zeta^{-7}\lambda^{-5}v_{n1}^{-4}k^2v_{n2}^{2}v_{P0}^{2}\tau_x^2\tau_y^2\tau_z^2(\tau_x^2 - 2\tau_y^2 + \tau_z^2), \quad \text{(C-42)}$$

$$\tau_{66} = -\frac{3}{2}\zeta^{-7}\lambda^{-5}k^2\tau_x^2(\tau_x^6 + 4\tau_x^4(\tau_y^2 + \tau_z^2) + 4\tau_y^4(\tau_y^2 + \tau_z^2) + 4\tau_x^2(\tau_y^4 + 3\tau_y^2\tau_z^2)), \quad \text{(C-43)}$$

$$\tau_{67} = 3\zeta^{-7}\lambda^{-5}v_{n2}^{-2}k^2v_{P0}^{2}\tau_x^2\tau_z^2(\tau_x^4 + 2\tau_x^2\tau_y^2 - 2\tau_y^4 - 2(\tau_x^2 + \tau_y^2)\tau_z^2), \quad \text{(C-44)}$$

$$\tau_{68} = i\zeta^{-7}\lambda^{-5}v_{n1}^{-2}kv_{n2}^{2}\tau_x^2\tau_y^2((1+ik)\tau_x^4 + (\tau_y^2 + \tau_z^2)((1+4ik)\tau_y^2 + (1-2ik)\tau_z^2) + 2\tau_x^2((1-2ik)\tau_y^2 + (1+4ik)\tau_z^2)), \quad \text{(C-45)}$$

$$\tau_{77} = -\frac{3}{2}\zeta^{-7}\lambda^{-5}v_{n2}^{-4}k^2v_{P0}^{4}\tau_x^2\tau_z^2(\tau_x^4 + \tau_x^2(\tau_y^2 - \tau_z^2) + \tau_z^2(\tau_y^2 + \tau_z^2)), \quad \text{(C-46)}$$

$$\tau_{78} = 3\zeta^{-7}\lambda^{-5}v_{n1}^{-2}k^2v_{P0}^{2}\tau_x^2\tau_y^2\tau_z^2(2\tau_x^2 - \tau_y^2 - \tau_z^2), \quad \text{(C-47)}$$

$$\tau_{88} = -\frac{3}{2}\zeta^{-7}\lambda^{-5}v_{n1}^{-4}k^2v_{n2}^{4}\tau_x^2\tau_y^2(\tau_x^4 - \tau_x^2\tau_y^2 + \tau_y^4 + (\tau_x^2 + \tau_y^2)\tau_z^2). \quad \text{(C-48)}$$

REFERENCES

Alkhalifah, T., 2003, An acoustic wave equation for orthorhombic anisotropy: Geophysics, **68**, 1169–1172, doi: 10.1190/1.1598109.

Alkhalifah, T., 2011, Scanning anisotropy parameters in complex media: Geophysics, **76**, no. 2, U13–U22, doi: 10.1190/1.3553015.

Amodei, D., H. Keers, W. Vasco, and L. Johnson, 2006, Computation of uniform wave forms using complex rays: Physical Review E, **73**, 1–14.

Batzle, M. L., D.-H. Han, and R. Hofmann, 2006, Fluid mobility and frequency-dependent seismic velocity: Direct measurements: Geophysics, **71**, no. 1, N1–N9, doi: 10.1190/1.2159053.

Behura, J., and I. Tsvankin, 2009, Estimation of interval anisotropic attenuation from reflection data: Geophysics, **74**, no. 6, A69–A74, doi: 10.1190/1.3191733.

Behura, J., I. Tsvankin, E. Jenner, and A. Calvert, 2012, Estimation of interval velocity and attenuation anisotropy from reflection data at Coronation Field: The Leading Edge, **31**, 580–587, doi: 10.1190/tle31050580.1.

Bender, C. M., and S. A. Orszag, 1978, Advanced mathematical methods for scientists and engineers: McGraw-Hill.

Ben-Menahem, A., and S. J. Singh, 1981, Seismic waves and sources: Springer.

Berryman, J. G., 1988, Seismic wave attenuation in fluid-saturated porous media: Pure and Applied Geophysics, **128**, 423–432, doi: 10.1007/BF01772607.

Best, A. I., J. Sothcott, and C. McCann, 2007, A laboratory study of seismic velocity and attenuation anisotropy in near-surface sedimentary rocks: Geophysical Prospecting, **55**, 609–625, doi: 10.1111/j.1365-2478.2007.00642.x.

Borcherdt, R. D., 2009, Viscoelastic waves in layered media: Cambridge University Press.

Carcione, J. M., 2015, Wave fields in real media: Theory and numerical simulation of wave propagation in anisotropic, anelastic, porous and electromagnetic media, 3rd ed.: Elsevier Handbook of Geophysical Exploration.

Carter, A. J., and J.-M. Kendall, 2006, Attenuation anisotropy and the relative frequency content of split shear waves: Geophysical Journal International, **165**, 865–874, doi: 10.1111/j.1365-246X.2006.02929.x.

Clark, R. A., P. M. Benson, A. J. Carter, and C. A. G. Moreno, 2009, Anisotropic P-wave attenuation measured from a multi-azimuth surface seismic reflection survey: Geophysical Prospecting, **57**, 835–845, doi: 10.1111/j.1365-2478.2008.00772.x.

Červený, V., 2001, Seismic ray theory: Cambridge University Press.

Červený, V., and I. Pšenčík, 2005a, Plane waves in viscoelastic anisotropic media. I: Theory: Geophysical Journal International, **161**, 197–212, doi: 10.1111/j.1365-246X.2005.02589.x.

Červený, V., and I. Pšenčík, 2005b, Plane waves in viscoelastic anisotropic media. II: Numerical examples: Geophysical Journal International, **161**, 213–229, doi: 10.1111/j.1365-246X.2005.02590.x.

Červený, V., and I. Pšenčík, 2006, Energy flux in viscoelastic anisotropic media: Geophysical Journal International, **166**, 1299–1317, doi: 10.1111/j.1365-246X.2006.03057.x.

Červený, V., and I. Pšenčík, 2009, Perturbation Hamiltonians in heterogeneous anisotropic weakly dissipative media: Geophysical Journal International, **178**, 939–949, doi: 10.1111/j.1365-246X.2009.04218.x.

Chapman, M., 2003, Frequency-dependent anisotropy due to meso-scale fractures in the presence of equant porosity: Geophysical Prospecting, **51**, 369–379, doi: 10.1046/j.1365-2478.2003.00384.x.

Chapman, M., 2009, Modeling the effect of multiple sets of mesoscale fractures in porous rock on frequency-dependent anisotropy: Geophysics, **74**, no. 6, D97–D103, doi: 10.1190/1.3204779.

Chapman, S. J., J. M. H. Lawry, J. R. Ockendon, and R. H. Tew, 1999, On the theory of complex rays: SIAM Review, **41**, 417–509, doi: 10.1137/S0036144599352058.

Dasgupta, R., and R. A. Clark, 1998, Estimation of Q from surface seismic reflection data: Geophysics, **63**, 2120–2128, doi: 10.1190/1.1444505.

Gajewski, D., and I. Pšenčík, 1992, Vector wavefields for weakly attenuating anisotropic media by the ray method: Geophysics, **57**, 27–38, doi: 10.1190/1.1443186.

Grechka, V., and I. Tsvankin, 1999, 3-D moveout inversion in azimuthally anisotropic media with lateral velocity variation: Theory and a case study: Geophysics, **64**, 1202–1218, doi: 10.1190/1.1444627.

Hanyga, A., and M. Seredyńska, 2000, Ray tracing in elastic and viscoelastic media: Pure and Applied Geophysics, **157**, 679–717, doi: 10.1007/PL00001114.

Hao, Q., and T. Alkhalifah, 2017, An acoustic eikonal equation for attenuating transversely isotropic media with a vertical symmetry axis: Geophysics, **82**, no. 1, C9–C20, doi: 10.1190/geo2016-0160.1.

Hao, Q., A. Stovas, and T. Alkhalifah, 2016, The offset-midpoint traveltime pyramid of P-waves in orthorhombic media: Geophysics, **81**, no. 5, C151–C162, doi: 10.1190/geo2015-0352.1.

Hearn, D. J., and E. S. Krebes, 1990a, On computing ray-synthetic seismograms for anelastic media using complex rays: Geophysics, **55**, 422–432, doi: 10.1190/1.1442851.

Hearn, D. J., and E. S. Krebes, 1990b,Complex rays applied to wave propagation in a viscoelastic medium: Pure and Applied Geophysics, **132**, 401–415, doi: 10.1007/BF00874371.

Jakobsen, M., and M. Chapman, 2009, Unified theory of global flow and squirt flow in cracked porous media: Geophysics, **74**, no. 2, WA65–WA76, doi: 10.1190/1.3078404.

Klimeš, L., 2002, Second-order and higher-order perturbations of travel time in isotropic and anisotropic media: Studia Geophysica et Geodaetica, **46**, 213–248, doi: 10.1023/A:1019802003257.

Klimeš, M., and L. Klimeš, 2011, Perturbation expansion of complex-valued traveltime along real-valued reference rays: Geophysics Journal International, **186**, 751–759, doi: 10.1111/j.1365-246X.2011.05054.x.

Kravtsov, Y. A., G. W. Forbes, and A. A. Asatryan, 1999, Theory and applications of complex rays, *in* E. Wolf, ed., Progress in optics: Elsevier, 1–62.

Krebes, E. S., and M. A. Slawinski, 1991, On ray tracing in an elastic-anelastic medium: Bulletin of the Seismological Society of America, **81**, 667–686.

Le, L. H. T., E. S. Krebes, and G. E. Quiroga-Goode, 1994, Synthetic seismograms for SH waves in anelastic transversely isotropic media: Geophysical Journal International, **116**, 598–604, doi: 10.1111/j.1365-246X.1994.tb03283.x.

Luo, S., and J. Qian, 2012, Fast sweeping methods for factored anisotropic eikonal equations: Multiplicative and additive factors: Journal of Scientific Computing, **52**, 360–382, doi: 10.1007/s10915-011-9550-y.

Masmoudi, N., and T. Alkhalifah, 2016, Traveltime approximations and parameter estimation for orthorhombic media: Geophysics, **81**, no. 4, C127–C137, doi: 10.1190/geo2015-0367.1.

Moczo, P., P.-Y. Bard, and I. Pšenčík, 1987, Seismic response of two-dimensional absorbing structures by the ray method: Journal of Geophysics, **62**, 38–49.

Quan, Y., and J. M. Harris, 1997, Seismic attenuation tomography using the frequency-shift method: Geophysics, **62**, 895–905, doi: 10.1190/1.1444197.

Rasolofosaon, P. N. J., 2010, Generalized anisotropy parameters and approximations of attenuations and velocities in viscoelastic media of arbitrary anisotropy type: Theoretical and experimental aspects: Geophysical Prospecting, **58**, 637–655, doi: 10.1111/j.1365-2478.2009.00863.x.

Sethian, J. A., 1996, A fast marching level set method for monotonically advancing fronts: Proceedings of the National Academy of Sciences of the United States of America, **93**, 1591–1595, doi: 10.1073/pnas.93.4.1591.

Sethian, J. A., and A. Vladimirsky, 2001, Ordered upwind methods for static Hamilton-Jacobi equations: Proceedings of the National Academy of Sciences, **98**, 11069–11074, doi: 10.1073/pnas.201222998.

Shekar, B., and I. Tsvankin, 2011, Estimation of shear-wave interval attenuation from mode-converted data: Geophysics, **76**, no. 6, D11–D19, doi: 10.1190/geo2010-0415.1.

Shekar, B., and I. Tsvankin, 2012, Anisotropic attenuation analysis of cross-hole data generated during hydraulic fracturing: The Leading Edge, **31**, 588–593, doi: 10.1190/tle31050588.1.

Stovas, A., 2015, Azimuthally dependent kinematic properties of orthorhombic media: Geophysics, **80**, no. 6, C107–C122, doi: 10.1190/geo2015-0288.1.

Stovas, A., N. Masmoudi, and T. Alkhalifah, 2016, Application of perturbation theory to a P-wave eikonal equation in orthorhombic media: Geophysics, **81**, no. 6, C309–C317, doi: 10.1190/geo2016-0097.1.

Tao, G., and M. S. King, 1990, Shear-wave velocity and Q anisotropy in rocks: A laboratory study: International Journal of Rock Mechanics and Mining Sciences and Geomechanics Abstracts, **27**, 353–361, doi: 10.1016/0148-9062(90)92710-V.

Thomsen, L., 1986, Weak elastic anisotropy: Geophysics, **51**, 1954–1966, doi: 10.1190/1.1442051.

Thomson, C. J., 1997, Complex rays and wave packets for decaying signals in inhomogeneous, anisotropic and anelastic media: Studia Geophysica et Geodaetica, **41**, 345–381, doi: 10.1023/A:1023359401107.

Tsai, Y.-H. R., L.-T. Cheng, S. Osher, and H.-K. Zhao, 2003, Fast sweeping algorithms for a class of Hamilton-Jacobi equations: SIAM Journal on Numerical Analysis, **41**, 673–694, doi: 10.1137/S0036142901396533.

Tsvankin, I., 1997, Anisotropic parameters and P-wave velocity for orthorhombic media: Geophysics, **62**, 1292–1309, doi: 10.1190/1.1444231.

van Trier, J., and W. W. Symes, 1991, Upwind finite-difference calculation of traveltimes: Geophysics, **56**, 812–821, doi: 10.1190/1.1443099.

Vavryčuk, V., 2006, Calculation of the slowness vector from the ray vector in anisotropic media: Proceedings of the Royal Society, Series A, **462**, 883–896, doi: 10.1098/rspa.2005.1605.

Vavryčuk, V., 2007, Ray velocity and ray attenuation in homogeneous anisotropic viscoelastic media: Geophysics, **72**, no. 6, D119–D127, doi: 10.1190/1.2768402.

Vavryčuk, V., 2008, Real ray tracings in anisotropic viscoelastic media: Geophysical Journal International, **175**, 617–626, doi: 10.1111/j.1365-246X.2008.03898.x.

Vavryčuk, V., 2009, Weak anisotropy-attenuation parameters: Geophysics, **74**, no. 5, WB203–WB213, doi: 10.1190/1.3173154.

Vavryčuk, V., 2010, Behavior of rays at interfaces in anisotropic viscoelastic media: Geophysical Journal International, **181**, 1665–1677.

Vavryčuk, V., 2012, On numerically solving the complex eikonal equation using real ray-tracing methods: A comparison with the exact analytical solution: Geophysics, **77**, no. 4, T109–T116, doi: 10.1190/geo2011-0431.1.

Vavryčuk, V., 2015, Determination of parameters of viscoelastic anisotropy from ray velocity and ray attenuation: Theory and numerical modeling: Geophysics, **80**, no. 3, C59–C71, doi: 10.1190/geo2014-0355.1.

Vidale, J. E., 1988, Finite-difference calculation of travel times: Bulletin of the Seismological Society of America, **78**, 2062–2076.

Vidale, J. E., 1990, Finite-difference calculation of traveltimes in three dimensions: Geophysics, **55**, 521–526, doi: 10.1190/1.1442863.

Waheed, U., C. Yarman, and G. Flagg, 2015, An iterative fast sweeping eikonal solver for 3-D tilted anisotropic media: Geophysics, **80**, no. 3, C49–C58, doi: 10.1190/geo2014-0375.1.

Winkler, K. W., and A. Nur, 1982, Seismic attenuation: Effects of pore fluids and frictional-sliding: Geophysics, **47**, 1–15, doi: 10.1190/1.1441276.

Zhang, Y.-T., H.-K. Zhao, and J. Qian, 2006, High order fast sweeping methods for static Hamilton-Jacobi equations: Journal of Scientific Computing, **29**, 25–56, doi: 10.1007/s10915-005-9014-3.

Zhu, T. F., and K. Y. Chun, 1994, Complex rays in elastic and anelastic media: Geophysical Journal International, **119**, 269–276, doi: 10.1111/j.1365-246X.1994.tb00927.x.

Zhu, Y., and I. Tsvankin, 2006, Plane-wave propagation in attenuative transversely isotropic media: Geophysics, **71**, no. 2, T17–T30, doi: 10.1190/1.2187792.

Zhu, Y., and I. Tsvankin, 2007, Plane-wave attenuation anisotropy in orthorhombic media: Geophysics, **72**, no. 1, D9–D19, doi: 10.1190/1.2387137.

Zhu, Y., I. Tsvankin, P. Dewangan, and K. van Wijk, 2007, Physical modeling and analysis of P-wave attenuation anisotropy in transversely isotropic media: Geophysics, **72**, no. 1, D1–D7, doi: 10.1190/1.2374797.

Zhubayev, A., M. E. Houben, D. M. J. Smeulders, and A. Barnhoorn, 2016, Ultrasonic velocity and attenuation anisotropy of shales, Whitby, United Kingdom: Geophysics, **81**, no. 1, D45–D56, doi: 10.1190/geo2015-0211.1.